Journal of Medicinal Chemistry



Article

# Synthesis and Evaluation of Asymmetric Acyclic Nucleoside Bisphosphonates as Inhibitors of Plasmodium falciparum and Human Hypoxanthine-Guanine-(Xanthine) Phosphoribosyltransferase

Petr Špa#ek, Dianne T. Keough, Marina Chavchich, Martin Dracinsky, Zlatko Janeba, Lieve Naesens, Michael D. Edstein, Luke W Guddat, and Dana Hocková

*J. Med. Chem.*, **Just Accepted Manuscript** • DOI: 10.1021/acs.jmedchem.7b00926 • Publication Date (Web): 16 Aug 2017



ACS Publications

Journal of Medicinal Chemistry is published by the American Chemical Society. 1155 Sixteenth Street N.W., Washington, DC 20036

# Synthesis and Evaluation of Asymmetric Acyclic Nucleoside Bisphosphonates as Inhibitors of *Plasmodium falciparum* and Human Hypoxanthine-Guanine-(Xanthine) Phosphoribosyltransferase

Petr Špaček,[a] Dianne T. Keough,[b] Marina Chavchich,[c] Martin Dračínský,[a] Zlatko Janeba,[a] Lieve Naesens,[d] Michael D. Edstein,[c] Luke W. Guddat,[b*] and Dana Hocková,[a*]

[a]*The Institute of Organic Chemistry and Biochemistry of the Czech Academy of Sciences, Flemingovo nám. 2, CZ-16610 Prague 6, Czech Republic*

[b]*School of Chemistry and Molecular Biosciences, The University of Queensland, Brisbane, Queensland, 4068, Australia*

[c]*Department of Drug Evaluation, Australian Army Malaria Institute, Enoggera, Brisbane, Queensland 4051, Australia*

[d]*KU Leuven - Rega Institute for Medical Research, Laboratory of Virology and chemotherapy Herestraat 49, B-3000 Leuven, Belgium*

**Keywords:** acyclic nucleoside phosphonates; phosphoramidate prodrugs; hypoxanthine-guanine-(xanthine) phosphoribosyltransferase, purine salvage pathway, malaria

**Abstract**

Acyclic nucleoside bisphosphonates (ANbPs) have previously been shown to be good inhibitors of human hypoxanthine-guanine phosphoribosyltransferase (HGPRT) and *Plasmodium falciparum (Pf)* hypoxanthine-guanine-xanthine phosphoribosyltransferase (*Pf*HGXPRT). Based on this scaffold, a new series of ANbPs was synthesized. One of these new ANbPs, [3-(guanine-9-yl)-2-((2-phosphonoethoxy)methyl)propoxy]methylphosphonic

acid, exhibited $K_i$ values of 6 and 70 nM for human HGPRT and *Pf* HGXPRT, respectively. These low $K_i$ values were achieved by inserting an extra carbon atom in the linker connecting the $N^9$ atom of guanine to one of the phosphonate groups. The crystal structure of this ANbP in complex with human HGPRT was determined at 2.0 Å resolution and shows that it fills three key pockets in the active site. The most potent phosphoramidate prodrugs of these compounds have $IC_{50}$ values in low micromolar range in *Pf l*ines and low toxicity in human A549 cells demonstrating that these ANbPs are excellent antimalarial drug leads.

## INTRODUCTION

Malaria remains as one of the most lethal infectious diseases known to afflict mankind with 429,000 deaths and 212 million infections in 2015.[1] The causative agent of malaria is a protozoan parasite that belongs to *Plasmodium* genus and is spread by the bite of female Anopheles mosquito. Of the five *Plasmodium* species that can infect humans, *Plasmodium falciparum (Pf)* and *Plasmodium vivax* (*Pv*) are the most lethal and widespread.[2] Artemisinin based combination therapies (ACTs) are used worldwide for the treatment of malaria, but alarmingly ACT resistance has emerged in Southeast Asia with failure rates of 50% and 26% in Cambodia[3] and Vietnam[4], with the use of dihydroartemisinin-piperaquine, respectively. On the basis that malarial infections remain as major cause of morbidity and mortality, the need to discover new antimalarial drug targets and new therapeutic agents with novel mechanisms is of the utmost importance.

Hypoxanthine-guanine-xanthine phosphoribosyltransferase (HGXPRT) is an attractive drug target for antimalarial drug therapy, as its activity is essential for both the survival and reproduction of malarial parasites.[5] This is because it provides the only pathway for the synthesis of the 6-oxopurine nucleoside monophosphates required for DNA and RNA production (salvage pathway). HGXPRT is also indirectly responsible for the synthesis of the

6-amino nucleoside monophosphate, AMP, as this is produced in these parasites starting from IMP. The nucleotides, IMP, GMP and XMP, are therefore synthesized from hypoxanthine, guanine and xanthine which are actively transported from their host cell. Though humans possess both a *de novo* pathway starting from simple precursors as well as the salvage pathway, the malarial parasites rely solely on the salvage pathway. Independent studies have shown that both purine starvation by inhibition of purine nucleoside phosphorylase[5] or hypoxanthine depletion[6] have been effective routes to preventing the growth of malarial parasites, either in cell culture or in Aotus monkeys. These data provide further confirmation that purine metabolism is a major flaw in the parasitic armory that can be exploited for effective antimalarial drug discovery.

HG(X)PRTs catalyse the formation of the 6-oxopurine nucleoside monophosphates from a nucleobase and from 5′-phospho-α-D-ribosyl-1-pyrophosphate (**Fig. 1**). The human and *Pv* enzymes use only hypoxanthine and guanine as substrates, whereas the *Pf* enzyme uses all three bases as substrates, hence the assignment of the enzymes as human HGPRT, *Pv*HGPRT and *Pf*HGXPRT. The presence of divalent metal ions, presumably magnesium *in vivo*, is essential for the reaction to proceed. Despite the fact that there is some redundancy in the salvage pathway (e.g. IMP dehydrogenase and GMP synthetase are present in the *Pf* genome), direct inhibition of HGXPRT[7,8] has been shown to be an efficient strategy for the development of novel lead antiparasitic and antibacterial agents.[9-15]

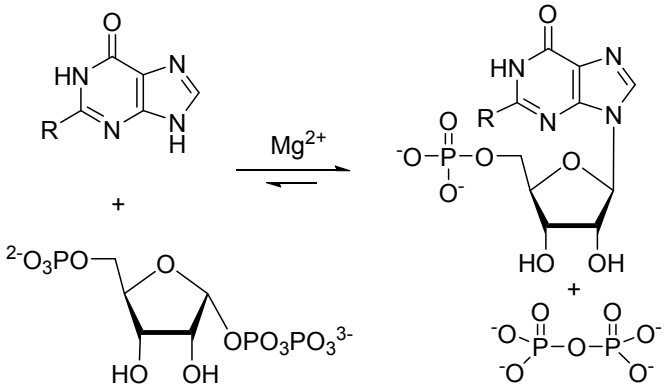

**Figure 1.** Reaction catalyzed by HGPRT/HGXPRT. R = H (hypoxanthine), R = $NH_2$ (guanine), R = OH (xanthine).

The chemical structures of bisphosphonate HGPRT/HGXPRT inhibitors[16] previously characterized in a SAR-study are given in **Figs. 2A** and **2B**. The basic structure of the newly synthesized ANbPs is shown in **Fig. 2C.**

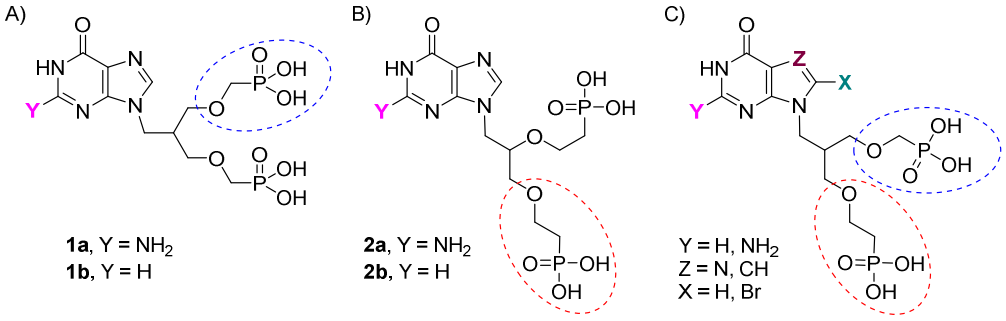


**Figure 2.** General structures of ANbP-based HGPRT/HGXPRT inhibitors: A) - B) previously published bisphosphonates[16]; C) new asymmetric inhibitors.

The design of new inhibitors presented in this paper (**Fig. 2C**) is based on alterations to the scaffold of published acyclic nucleoside bisphosphonates (ANbPs, **Fig. 2AB**). These ANbPs have a 6-oxopurine base attached either to a symmetric moiety bearing two phosphonomethyloxy groups (**Fig. 2A**) or to an asymmetric moiety with two phosphonoethyloxy groups (**Fig. 2B**).[16] The rationale for the design of new asymmetric ANbPs (**Fig. 2C**) is based on the crystal structure of human HGPRT in complex with **1a** (**Fig. 2A** and **Fig. 3**).[16] In new series of compounds, five atoms[17] are contained in the linker connecting the $N^9$ atom of the purine base with one of the phosphonate groups. The crystal structure of human HGPRT in complex with **1a**[16] shows that this particular phosphonate group is located in the 5′-phosphate binding pocket (**Fig. 3**). The second phosphonate group

points down towards the $PP_i$ binding pocket but this moiety is not located in this pocket. Instead, a sulphate ion, from the crystallization buffer, was found to occupy this site which is also the location where the second product of the reaction, $PP_i$, binds. The crystal structure shows that a magnesium ion is coordinated to one of the sulphate oxygen atoms and one of the phosphonate oxygen atoms of **1a** (**Fig. 3**).[16]

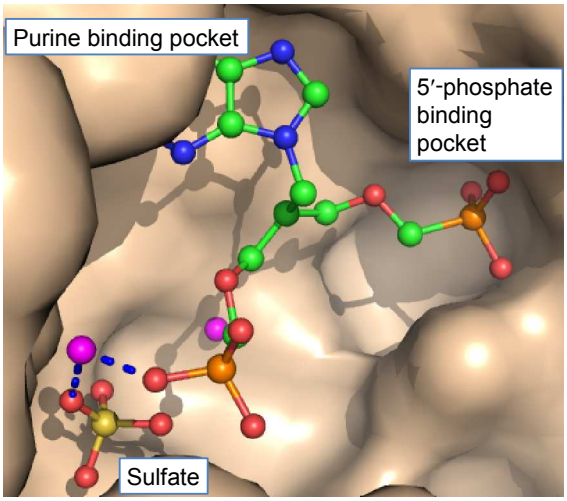


**Figure 3.** [(2-[(guanin-9-yl)methyl]propane-1,3-diyl)bis(oxy)]bis(methylene)diphosphonic acid (**1a**) bound in the active site of human HGPRT (Protein Data Bank coordinates 4IJQ).[16] A sulphate ion from the crystallization media is present in the complex along with two magnesium ions (purple spheres).

Molecular docking suggested that lengthening one of the linkers by one atom may allow the second phosphonate group to be located in the $PP_i$ binding pocket leading to decreased $K_i$ values (**Fig. 4** yellow structure). In addition, the chemical nature of the purine base was altered to examine the effects of such changes on the inhibition constants for human HGPRT and *Pf*HGXPRT.

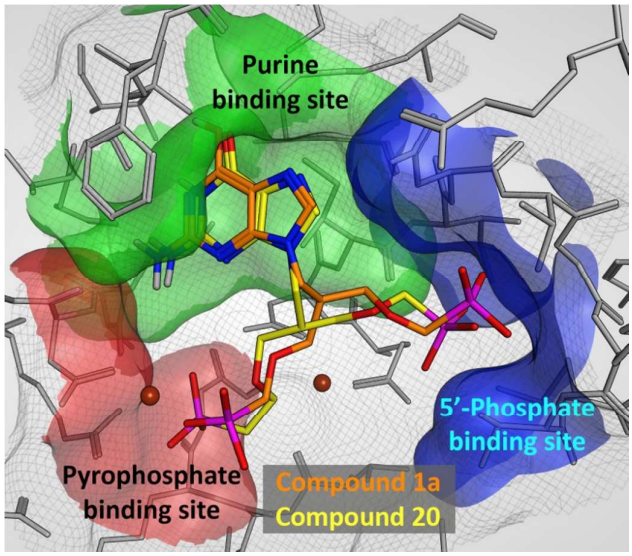


**Figure 4.** Comparison of the crystal structure of the human HGPRT. **1a** complex[16] with the docked structure of the new guanine derivative, **20** (**Scheme 2**), overlaid.

To test the antimalarial activity of the new inhibitors in erythrocyte cell culture infected by *Pf*, a prodrug approach was employed.[18] The highly polar bisphosphonates are unable to cross the cell membrane unless the phosphonate groups are masked by moieties which are cleaved enzymatically once the intact prodrug enters the cells. Phosphoramidate prodrugs bearing four non-toxic ethyl ester of L-phenylalanine moieties[14,16,19] were prepared, their $IC_{50}$ values measured against *Pf* in cell culture and their cytotoxicity in mammalian cells in tissue culture determined.

## RESULTS AND DISCUSSION

### 2.1. Chemistry

The synthesis of this series of asymmetric ANbPs inhibitors can be described in three consecutive parts. The first part was to prepare the key hydroxy derivative **8**. This precursor contains two different functional groups – phosphonomethyl and phosphonoethyl – attached

via ether bonds to the main scaffold (**Scheme 1**). The second part of the synthesis was the Mitsunobu reaction affording the connection of this bisphosphonate moiety to N-9 position of a purine base. The last part was a sequence of reactions transforming the preformed derivatives to the final inhibitors (**Scheme 2**).

Starting material **3** (5-hydroxymethyl-2,2-dimethyl-1,3-dioxane) was prepared by simultaneous protection of two hydroxy groups of commercially available 2-hydroxymethyl-1,3-propanediol using reaction with dry acetone and acid catalyst.[20] Obtained alcohol **3** was transformed to a phosphonomethyloxy derivative **4** by the reaction with diisopropyl (bromomethyl)phosphonate and sodium hydride in DMF. Intermediate **4** was treated with DOWEX (50WX8 $H^+$) in methanol to obtain dihydroxy derivative **5**, which was a key intermediate for the subsequent synthetic pathways (**Scheme 1**).

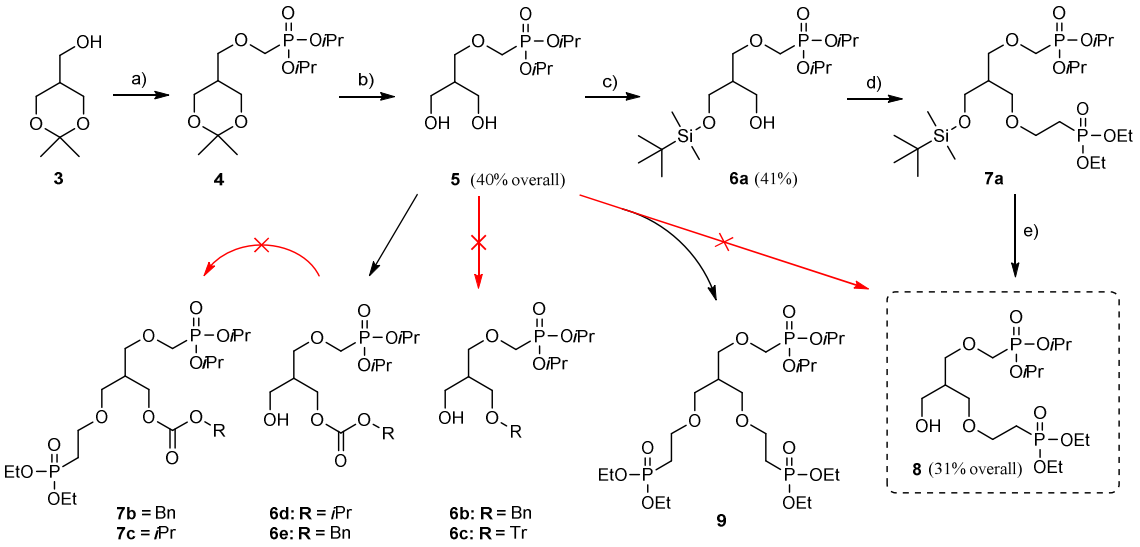


**Scheme 1**: a) $BrCH_2P(O)(OiPr)_2$, NaH, DMF, 0°C; b) DOWEX (50WX8 $H^+$), 90% MeOH, 50°C; c) TBDMSCl, imidazole, DMF, r.t.; d) Diethyl vinylphosphonate, $Cs_2CO_3$, *t*-BuOH, r.t.; e) DOWEX (50WX8 $H^+$), 90% MeOH, 50°C.

In the course of the first attempts to attach the second phosphonate group, dihydroxy derivative **5** was treated with various molar equivalents of diethyl vinylphosphonate under oxa-Michael reaction conditions.[21] However, required alcohol **8** was not obtained in a sufficient quantity. Depending on the reaction conditions (using various bases and differing amounts of diethyl vinylphosphonate), we observed either product **9** with two attached phosphonoethoxy groups or the starting material **5** with a very small amount of desired product **8**. Therefore, we tried to protect one of the hydroxy groups of intermediate **5** using standard protecting groups. This would subsequently enable a selective introduction of only one phosphonoethoxy group. Experiments with several alkylating agents (benzyl halogenides or trityl chloride) under various reaction conditions (low temperature, various dry solvents, different bases) were carried out. Unfortunately, none of these methods to synthesize derivatives **6b** and **6c** were successful on a preparative scale.

Another approach was to prepare a fully protected cyclic carbonate diester derivative from dihydroxy phosphonate **5** using ethyl chloroformate in THF with the addition of triethylamine, and subsequently cleave this compound by an acid-catalysed reaction with silica gel and corresponding alcohol to form carbonate esters **6d** and **6e**. Isopropyl alcohol and benzyl alcohol were chosen to diversify possible methods for later deprotection. Attempts were then made to attach a phosphonoethoxy functional group to intermediates **6d** or **6e**. Despite multiple attempts with reaction conditions of oxa-Michael addition, phosphonoethoxy derivatives **7b** and **7c** could not be obtained.

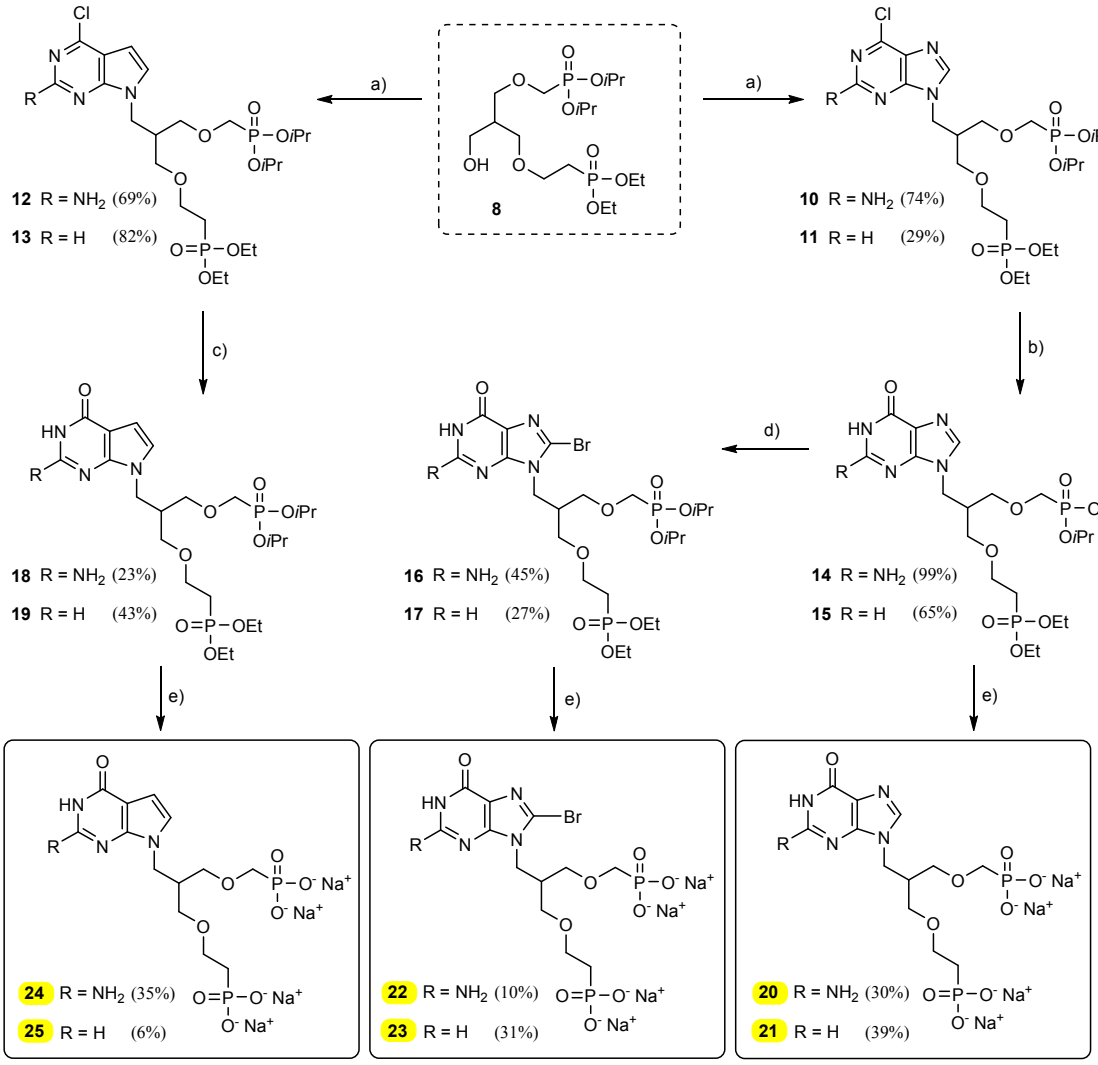


**Scheme 2**: a) DIAD, $PPh_3$, 6-chloropurine, 2-amino-6-chloropurine or corresponding 7-deazapurines, THF, -30°C; b) $CF_3COOH$, $H_2O$, r.t.; c) $K_2CO_3$, DABCO, $H_2O$, 120°C; d) $Br_2$, $CCl_4$, DMF, r.t.; e) $BrSi(CH_3)_3$, $CH_3CN$, r.t.

Ultimately, a successful synthetic pathway was developed (**Scheme 1**). This was via a *tert*-butyldimethylsilyl protected intermediate **6a**, which was prepared by the reaction of a 1.1 molar equivalent of *tert*-butyldimethylsilyl chloride (TBDMSCl) and imidazole as a base in THF.[22] Protected alcohol **6a** further reacted with diethyl vinylphosphonate under standard reaction conditions of oxa-Michael addition to form bisphosphonate **7a**. Intermediate **7a** was

treated with DOWEX (50WX8 $H^+$) to obtain the final hydroxy derivative **8,** a key precursor for the synthesis of the inhibitors and their prodrugs.

Further process leading to the synthesis of asymmetrical ANbPs was based on parallel reaction procedures (**Scheme 2**). First, bisphosphonate moiety of alcohol **8** was introduced under Mitsunobu reaction conditions to the N-9 position of 2-amino-6-chloropurine, 6-chloropurine, 2-amino-6-chloro-7-deazapurine and 6-chloro-7-deazapurine to form derivatives **10**, **11**, **12**, **13**. Transformation to the corresponding 6-oxopurine and 6-oxo-7-deazapurine analogues followed. 6-Chloropurine derivatives **10** and **11** were treated using standard conditions with a mixture of trifluoroacetic acid and water to obtain intermediates **14** and **15**.[16] For intermediates **12** and **13** with 7-deaza-modified heterocyclic bases a more vigorous method had to be applied. Thus, 7-deazapurine compounds **12** and **13** were hydrolysed by the reaction with potassium carbonate and DABCO in water[17,23] to form 6-oxo-7-deazapurine derivatives **18** and **19**.

Previously, an activity of several 8-bromoguanine derivatives was observed.[24] Therefore we also decided to prepare bromo derivatives for testing. Thus, intermediates **14** and **15** were used for preparation of bromo derivatives **16** and **17** by bromination with elementary bromine in $CCl_4$ and DMF. Synthesis of bromo derivative **27** started from a previously published[16] diester of bisphosphonate **2c** , which was transformed to the corresponding 8-bromoguanine derivative **26** by the above mentioned bromination method (**Scheme 3)**.

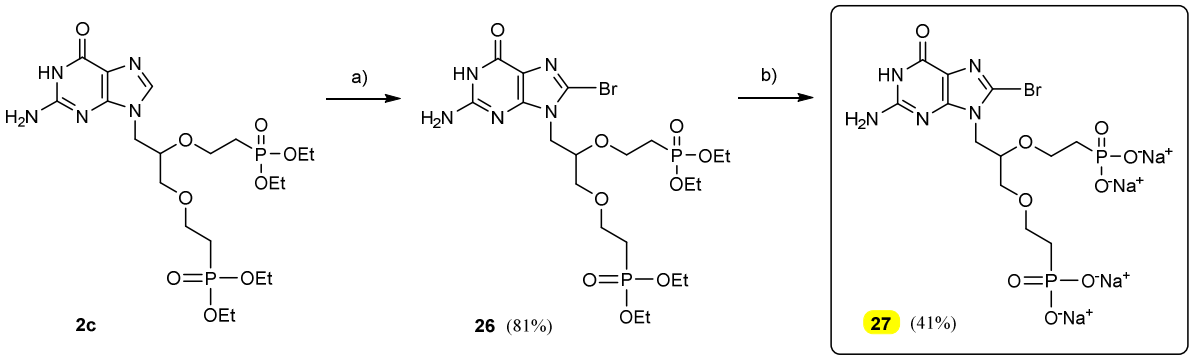


**Scheme 3**: a) $Br_2$, $CCl_4$, DMF, r.t.; b) $BrSi(CH_3)_3$, $CH_3CN$, r.t.

The last step for the preparation of the target ANbPs was the cleavage of phosphonate ester groups.[25] Esters **14**, **15**, **16**, **17**, **18, 19** and **26** were treated with bromotrimethylsilane in acetonitrile followed by hydrolysis to obtain free phosphonic acids **20**, **21**, **22**, **23**, **24, 25** and **27.**

To improve cell penetration properties of the ANbP inhibitors, phosphoramidate prodrugs were prepared from corresponding esters (**Scheme 4**). Phosphonate ester precursors **14**, **15**, **18** and **19** were transformed to the corresponding prodrugs **28**, **29**, **30** and **31** by treatment with bromotrimethylsilane in acetonitrile, followed by the reaction of thus preformed silyl esters with *L*-phenylalanine ethyl ester, 2,2′-dipyridyl disulfide and triphenylphosphine in dry pyridine.[16,26]

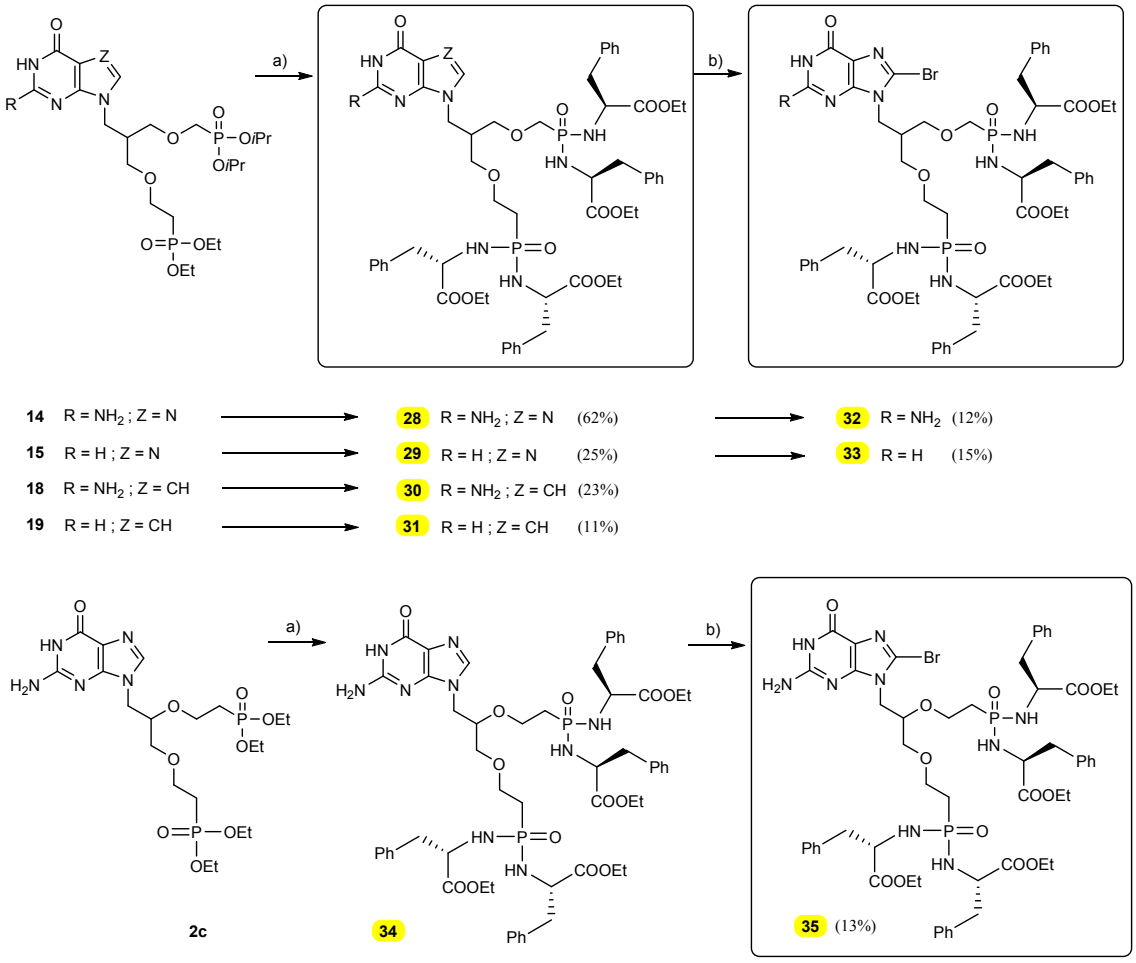


**Scheme 4**: a) 1. $BrSi(CH_3)_3$, $CH_3CN$, r.t, 2. $PPh_3$, Aldrithiol, (L)-$NH_2CH(Bn)COOEt.HCl$, $Et_3N$, pyridine, 70°C; b) NBS, 1,4-dioxane, MW, 100°C.

Direct preparation of phosphoramidate prodrugs of 8-bromo ANbPs from the corresponding esters is not possible.[20] Therefore direct bromination of the final prodrugs with NBS and 1,4-dioxane in a microwave reactor was used. Using this approach, prodrugs **28**, **29** and previously published[16] prodrug **34** were transformed to corresponding 8-bromopurine prodrugs **32**, **33** and **35** (**Scheme 4**).

## 2.2. Inhibition of human HGPRT and *Pf* HGXPRT

The $K_i$ values of the newly synthesized ANbPs for human HGPRT and *Pf*HGXPRT are given in **Table 1** together for the data obtained with the previously published compounds (**1a**, **1b** and **2a**; **Figs. 2A** and **2B**)[16] to allow a direct comparison.

**Table 1:** Summary of $K_i$ values for ANbPs with human HGPRT and *Pf* HGXPRT.

| No. | Base | Acyclic moiety | human HGPRT $K_i$ [μM] | *Pf*HGXPRT $K_i$ [μM] |
|---|---|---|---|---|
| | | **Series 1** | | |
| **1a** | G | | 0.03 ± 0.002[a] | 0.07 ± 0.01[a] |
| **1b** | Hx | 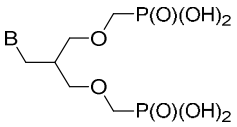 | 1 ± 0.1[a] | 5 ± 1[a] |
| | | **Series 2** | | |
| **2a** | G | | 0.6 ± 0.02[a] | 0.5 ± 0.01[a] |
| **2b** | Hx | | 0.7 ± 0.1 | NI[b] |
| **27** | 8-Br-G | 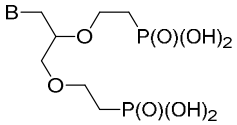 | 0.4±0.2 | 0.9±0.3 |
| | | **Series 3** | | |
| **20** | G | | 0.006 ± 0.001 | 0.07±0.05 |
| **21** | Hx | | 1.8±0.6 | 3±1 |
| **22** | 8-Br-G | | 0.1 ± 0.03 | 2±1 |
| **23** | 8-Br-Hx | 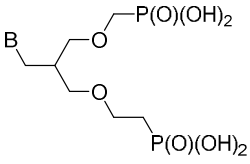 | 2.5 ± 1 | NI[c] |
| **24** | 7-deaza-G | | 0.1±0.5 | 4±2 |
| **25** | 7-deaza-Hx | | 4.6 ± 2 | 6±3 |

[a]Data from Ref. 16.

[b,c]No inhibition for **2b** and **23** was observed when these compounds were tested at a concentration of 33 μM and 50 μM, respectively.

Compound **1a** is a potent inhibitor of both the human and *Pf* enzymes (**Table 1)**.[16] Surprisingly, changing the attached purine base from guanine to hypoxanthine resulted in a large increase in $K_i$ values (33-fold for human HGPRT and 71-fold for *Pf*HGXPRT). This is partly understandable for the human enzyme as guanine has a two-fold lower $K_m$ for guanine compared with hypoxanthine (1.9 μM for guanine compared with 3.4 μM for hypoxanthine). The *Pf* enzyme, on the other hand, has a lower $K_m$ value for hypoxanthine compared with guanine (0.8 μM for guanine compared with 0.07 μM for hypoxanthine).[24] The significant increase in the $K_i$ value due to the change in the base from guanine to hypoxanthine is evident when the $K_i$ values of **20** and **21** are compared resulting in a 300-fold increase for human HGPRT and a 43-fold increase for *Pf*HGXPRT. Thus, for these two ANbP scaffolds, the nature of the purine base, whether hypoxanthine or guanine, has a significant influence on the $K_i$ values.

In **Series 2**, substitution of guanine by hypoxanthine had little effect on the $K_i$ values for the human enzyme (0.4-0.7 μM) (**Table 1**) though, once again, a large increase was observed for *Pf*HGXPRT. In this series, there was no change in the $K_i$ value when guanine was replaced by 8-bromoguanine for either enzyme. The only difference in the structures in the ANbPs in **Series 2** compared with **Series 3** is the position of the oxygen atom in the linker (**Table 1**). Thus, the higher $K_i$ values for the guanine containing compounds in **Series 2** compared with **Series 3** is attributed to the change in position of this oxygen atom. This atom is located in the linker connecting the $N^9$ atom of the base with the phosphonate group predicted to bind in the 5′-phosphate binding pocket. This prediction is based on the crystal structure of the human HGPRT.**1a** complex (**Fig. 3**).[16] The location of the oxygen atom can

influence the conformation of the linker and, thus, the location of the phosphonate group and the purine base in the active site. Therefore, it is clear that subtle chemical modifications can have a large effect on the orientation of the ANbPs in the active site.

In **Series 3**, the attachment of 8-bromo- or 7-deaza bases, either guanine or hypoxanthine derivatives, resulted in weak inhibition of both enzymes. Both these bases are very weak substrates and this, obviously, influences the affinity of their ANbP. The crystal structure of **20** (**Series 3**) in complex with human HGPRT was obtained and compared with that of the human HGPRT.**1a** structure to explain the decrease in the $K_i$ values (*cf.* **Series 3** and **Series 1**). This structure also provides an entry into the design of next generation compounds based on the structure and activity of these ANbPs.

**2.3. The crystal structure of the human HGPRT.20 complex.**

To explain the potent binding of **20,** the crystal structure of the human HGPRT.**20** was determined to 2.03 Å resolution. The refinement statistics of this structure are given in **Table 2**. The crystals contains a tetramer in the asymmetric unit (**Table 2**) and **20** is bound in the active site of each subunit (**Figure 5**). **Figure 5** shows that the large mobile loop of ~20 amino acid residues is disordered. This compares with its structure when ImmGP[27]/ImmHP[8] /acyclic immucillin phosphonate (AIP)[10], $PP_i$ and $Mg^{2+}$ are bound to human HGPRT or to *Pf*HGXPRT where this region becomes ordered and closes over the active site. The immucillins are compounds that are inert mimics for the predicted transition state of the reaction (**Fig. 1**). When AIP binds, the large mobile loop becomes ordered and covers the active site of *Pf*HGXPRT. The ordering is due to the formation of hydrogen bonds between (i) the backbone amide S115 (*Pf* numbering) and a pyrophosphate oxygen, (ii) the backbone amide of Y116 (*Pf* numbering) and the same pyrophosphate oxygen and (iii) the hydroxyl of

Y116 and a phosphonate oxygen of AIP. Similar sets of stabilizing interactions have also been observed when ImmGP or ImmHP bind to human HGPRT or *Pf*HGXPRT.[8,27]

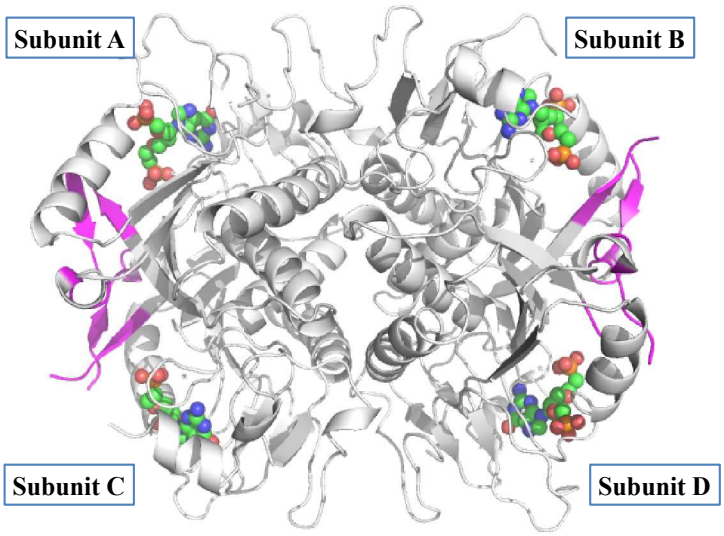


**Figure 5.** Crystal structure of the tetrameric human HGPRT.**20** complex. Magenta highlights the location of the ordered regions adjacent to the large mobile loop, residues R100-D120, which are not visible in this complex.

**Table 2. Data collection and refinement statistics for the human HGPRT.20 complex.**

| | |
|---|---|
| *Crystal parameters* | |
| *a, b, c* (Å) | 56.67, 128.40, 65.33 |
| α, β, γ (°) | 90.0, 103.0, 90.0 |
| Space group | $P\,2_1$ |
| Crystal size (mm) | 0.3 x 0.1 x 0.05 |
| Resolution range (Å) | 47.30 - 2.03 |
| Observations | 438 819 (31 172) |
| Unique reflections | 58 747 (4 242) |
| Completeness (%) | 99.7 (98.1) |
| $^{b}R_{merge}$ | 0.081 (0.654) |

| | |
|---|---|
| [c]$R_{p.i.m.}$ | 0.038 (0.277) |
| <I>/<σ(I)> | 13.9 (2.2) |
| Resolution limits (Å) | 47.30 – 2.35 |
| $R_{work}$ | 0.1962 |
| $R_{free}$ | 0.2487 |
| [d]Clashscore | 11.0 |
| *RMSD* | |
| Bond lengths (Å) | 0.0036 |
| Bond angles (°) | 0.713 |
| Tetramers | 1 |
| Inhibitors | 4 |
| Waters | 521 |
| $Mg^{2+}$ | 4 |
| Favoured | 96.91 |
| Outliers | 2.33 |

[a]Values in parentheses are for the outer resolution shell (2.08-2.03 Å). All data were collected at 100 K.

$$R_{merge} = \sum_{hkl}\sum_i \left|I_i(hkl) - \left(I(hkl)\right)\right| / \sum_{hkl}\sum_i I_i(hkl)$$

$$R_{p.i.m.} = \sum_{hkl} \left[\frac{1}{[N(hkl)-1]}\right]^{1/2} \sum_i \left|I_i(hkl) - \left(I(hkl)\right)\right| / \sum_{hkl}\sum_i I_i(hkl)$$

where $I_i(hkl)$ is the observed intensity and $I(hkl)$ is the average intensity obtained from multiple observations of symmetry related reflections. [d]Clashscore is defined as the number of bad overlaps ≥ 0.4 Å per thousand atoms.

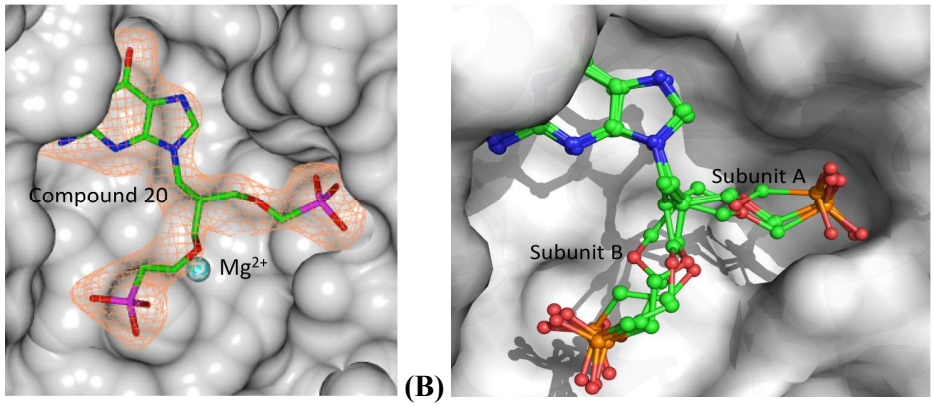


**Figure 6. (A)** Electron density map of [3-(guanine-9-yl)-2-((2-phosphonoethoxy)methyl)propoxy]methylphosphonic acid (**20**) bound in subunit C. The pale blue sphere shows the location of the single magnesium ion in the active site. (**B**) Superimposition of subunits, A, B, C and D showing the location of **20** in each of the four active sites.

**Figure 6A** shows the electron density for **20** in the active site and **Figure 6B**, the superimposition of the structure of the inhibitor bound in each of the four subunits. The location of the three critical structural elements of **20** *i.e.* the purine ring and the two phosphonate groups are the same in each of the four subunits, though there are slight differences in the conformation of the linker (**Fig. 6B**). The only significant difference occurs in subunit B. In this subunit, the oxygen atom is pushed further back into the active site than in the other three subunits. In this position, it is located within 2.5 Å of a water molecule that forms a hydrogen bond to the $N^3$ of the purine ring (**Fig. 7**). This water molecule also forms a hydrogen bond to one of the phosphonyl oxygen atoms. There are no interactions between either of the two linkers and active site residues or bridging waters.

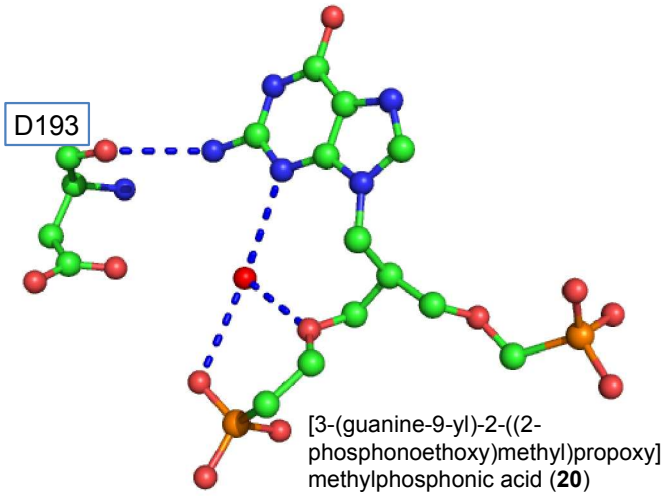


**Figure 7.** The interaction between the oxygen atom in one of the linkers and the bridging water molecule when **20** is bound in the active site of subunit B of human HGPRT**.** The hydrogen bond between the exocyclic amino group and the carbonyl of D193 occurs in all subunits.

***Comparison of the crystal structures of the human HGPRT.1a and HGPRT.20 complexes***. Superimposition of these two structures reveals that the location of the purine base and the phosphonate group bound in the 5′-phosphate binding pocket are identical (**Fig. 8**) and that the structure of the flexible loops that surround the active site are unchanged (**Fig. 8**). The differences between the two structures is in the location of the second phosphonate group (**Fig. 8**).

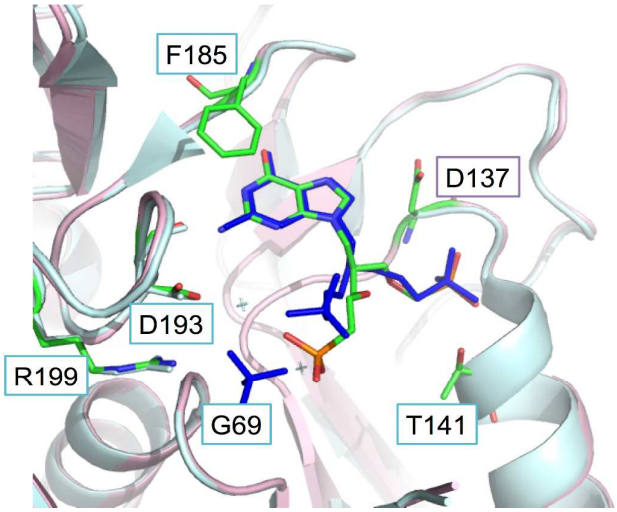


**Figure 8.** Comparison of the binding mode of **20** and **1a** (PDB code: 4IJQ) in the active site of human HGPRT. Compound **1a** with the associated sulfate ion (dark blue); Compound **20** (colored by element).

Thus, the differences in the $K_i$ values between **20** and **1a** for human HGPRT are attributed to how the second phosphonate group which points down into the $PP_i$ pocket binds in the active site. In the human HGPRT.**20** complex, this group points back into the active site towards the $PP_i$ binding pocket while, in **1a**, it points out of the active site leaving room for a sulfate and magnesium ion to bind (**Fig. 8**). It is, therefore, speculated that the higher $K_i$ value for *Pf*HGXPRT compared to human HGPRT (**Table 1**) may be due to differences in the mode of binding of this phosphonate group.

***The specific interactions that the phosphonyl oxygens of the second phosphonate group form at the active site in the human HGPRT.20 complex.*** A network of hydrogen bonds holds this phosphonate group in place when **20** is bound in the active site of human HGPRT (**Fig. 8**). One of the phosphonyl oxygen atoms forms hydrogen bonds to three water molecules. These form hydrogen bonds with each other and with the highly conserved residues, D193 (OD), R199 ($NH_2$) and G69 (backbone nitrogen). A second hydrogen bond is also evident between one of the other phosphonyl oxygen atoms and a water molecule that

forms a hydrogen bond with the OD atom of D134 and is also coordinated to a magnesium ion (**Fig. 9**). Thus, this network of bonds via bridging waters makes a strong contribution to anchoring **20** in position.

In the human HGPRT.**20** complex, the phosphonate group (**Fig. 9)** is located in the same position as one of phosphate groups of pyrophosphate when this second product of the reaction is bound in the active site of human HGPRT together with ImmGP[27] and magnesium ions (**Fig. 10**). The space in the active site occupied by the second phosphate group of $PP_i$ is, instead, occupied by water molecules when **20** binds (*cf.* **Figs. 9** and **10**). In the human HGPRT.**1a** complex), sulfate ions replaces one of the phosphate group of $PP_i$ **(Fig. 10).** As there are no negatively charged ions in this vicinity in the human.**20** complex *i.e.* phosphate or sulfate, the magnesium ion found in the HGPRT.ImmGP.PPi and HGPRT.**1a** complexes is not present.

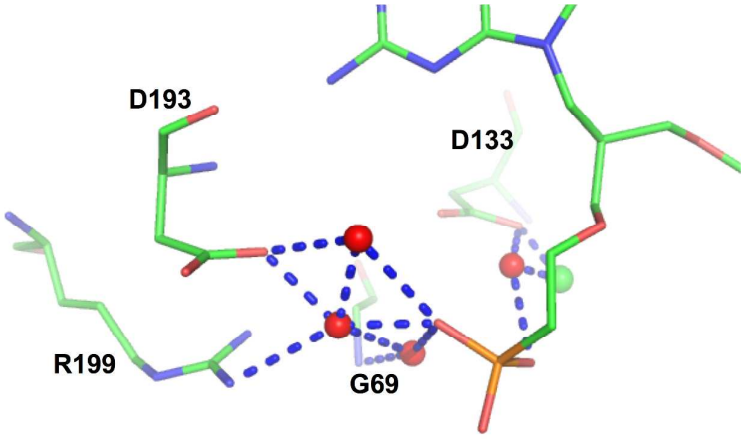


**Figure 9.** The network of hydrogen bonds that the phosphonyl oxygen atoms of the phosphonate groups which points into the $PP_i$ binding pocket forms at the active site of the human HGPRT.**20** complex. The green sphere is magnesium ion and the red spheres are waters.

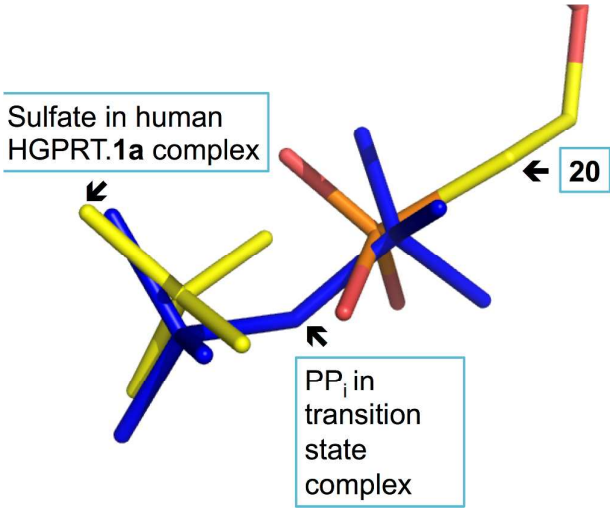


**Figure 10.** Superimposition of the human HGPRT.**20** complex with the human enzyme in complex with (2-[(guanin-9-yl)methyl]propane-1,3-diyl)bis(oxy)]bis(methylene)diphosphonic acid (**1a**) and sulfate (yellow)[16] (PDB code: 4IJQ) and ImmGP and pyrophosphate (dark blue)[27] (PDB code: 1BZY).

The network of hydrogen bonds is a strongly contributing factor leading to the low $K_i$ value of **20** for human HGPRT. It is unclear though why the hypoxanthine derivative binds much more weakly to both the human and *Pf* enzymes (**Table 1**). The absence of a single hydrogen bond between the backbone carbonyl of D193 and the exocyclic amino group seems unlikely to cause such a dramatic decrease if the ANbP was bound in exactly the same place as its guanine counterpart. Thus, the most logical conclusion is that this is not the case and, when the base is hypoxanthine, this change influences the whole orientation of the ANbP in the active site and, thus, has a much higher $K_i$ value.

**2.4. *In vitro* antimalarial study in erythrocyte cell cultures infected by *Plasmodium falciparum***. Phosphoramidate prodrugs (**Scheme 4**) for each inhibitor in **Table 1** were synthesized and tested for their ability to restrict the growth of *Pf* in cell culture. The results are given in **Table 3**.

**Table 3:** *In vitro* antimalarial activity and cytotoxicity of ANbP prodrugs in cell culture assays.

| Compound | | **Y** = $CH(CH_2Ph)COOEt$ | $IC_{50}$ (μM) | | $CC_{50}$ (μM) | SI |
|---|---|---|---|---|---|---|
| **No.** | Base | Acyclic moiety | D6[a] | W2[b] | A549[c] | D6/A549 |
| **36** | G | **Series 1** 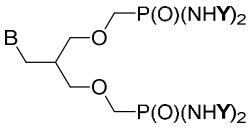  | 9.7 ± 1.6[d] | 7.1 ± 2.1[d] | >300[d] | >30 |
| **37** | Hx | | 3.8 ± 0.5[d] | 4.0 ± 0.9[d] | 101 ± 17[d] | 27 |
| **34** | G | **Series 2** 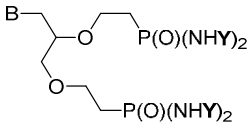  | 6.6 ± 2.3[d] | 7.7 ± 1.4[d] | 107 ± 55[d] | 16 |
| **38** | Hx | | 3.6 | 1.9 | 90 ± 29 | 25 |
| **35** | 8-Br-G | | ND | ND | 188 ± 43 | - |
| **28** | G | **Series 3** 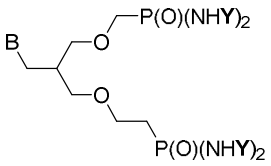  | 5.7 ± 0.3 | 7.4 ± 0.7 | 212 ± 16 | 37 |
| **29** | Hx | | 1.4 ± 0.2 | 3.2 ± 0.5 | 82 ± 11 | 59 |
| **32** | 8-Br-G | | 5.6 ± 0.1 | 8.3 ± 1.2 | 151 ± 27 | 27 |
| **33** | 8-Br-Hx | | ND | ND | 36 ± 5 | - |
| **30** | 7-deaza-G | | 1.8 ± 0.0 | 6.5 ± 2.6 | 106 ± 23 | 59 |
| **31** | 7-deaza-Hx | | ND | ND | 20 ± 4 | - |

B = purine base; ND = not determined [a] *Pf* strain sensitive to most drugs; [b] Chloroquine- and pyrimethamine-resistant *Pf* strain; [c] Human lung carcinoma cells; [d] Data from Ref. 16. SI = selectivity index = $CC_{50}/IC_{50}$. $IC_{50}$ and $CC_{50}$ represent the concentrations of the drug where cell growth is reduced by 50% in *Pf* and human cells, respectively

The $IC_{50}$ values range between 1.4-9.7 μM. The precise reason for the variability is unknown as it could be attributed to a number of factors. These include differences in transport across the plasmodial membrane and/or hydrolysis of the prodrug to its active

component. The phosphoramidate prodrugs have several advantages: They have a long intracellular half-life that allows infrequent dosing, the nontoxic amino acid moieties serve as an attachment and their properties can be fine-tuned, and there is no stereochemistry issue (in contrast to Pro-Tide approach). Thus, the phosphoramidates can serve as good model compounds to show the *in vitro* activity of inhibitors and to compare individual types of inhibitors with each other. An encouraging result is the fact that **28**, whose parent compound **20** is the most potent inhibitor of human HGPRT ($K_i$ = 6 nM), has an extremely low cytotoxicity in human A549 cell line. This is also true for compound **36**. It confirms the assumption that HGXPRT is an excellent drug target based on the fact that the purine salvage pathway is much more important for the parasite than for its host. Further studies are in progress to investigate if modifications to these current prodrugs can improve antimalarial activity.

## CONCLUSIONS

The new ANbPs exhibit a range of $K_i$ values for human HGPRT (0.006-4.6 μM) and for *Pf*HGXPRT (0.07-6.0 μM). These values strongly depend on the nature of the purine base. The crystal structure of the most potent of these inhibitors in complex with human HGPRT has been obtained. This suggests that one of the factors that could contribute to the potency and/or the selectivity for human HGPRT and *Pf*HGXPRT could be the binding of one of the phosphonate groups in the binding pocket of the second product of the reaction, $PP_i$. Variable micromolar antiparasitic activity of phosophoramidate prodrugs of these inhibitors in *Pf* infected erythrocyte cultures was observed. The toxicity data in human cell line show that even a prodrug (**28**) of potent inhibitor of human HGPRT (**20**) does not affect host cells, but at the same time can be toxic to parasites.

## EXPERIMENTAL SECTION

**Synthesis and Analytical Chemistry**. Unless stated otherwise, solvents were evaporated at 40°C/2 kPa, and compounds were dried in vacuum oven at 2 kPa. Tetrahydrofuran (THF) was distilled with lithium aluminium hydride pellets under argon. *Tert*-Butanol was stored over annealed molecular sieves (4 Å).

$^{1}$H and $^{13}$C NMR spectra were measured on a Avance 500 spectrometer (500 MHz and 126 MHz) in DMSO-*d6*, $D_2O$ or $D_2O$-(NaOD additive) and referred to TMS, residual solvent signal or added solvent (tBuOH or 1,4-dioxan). Complete assignment is based on heteronuclear correlation experiments HSQC and H, C-HMBC. Chemical shifts ($\delta$) are in ppm and coupling constants ($J$) in Hz. The numbering system for the assignment of NMR signals is described in **Fig. 11**. GC/MS spectra were measured on Agilent 5975B MSD spectrometer coupled to 6890N gas chromatograph. Determination of low-resolution mass spectra is described below (procedure 1 a procedure 2). High resolution mass spectra were measured: on Q-Tof micro (Waters) using ESI technique for low-resolution mass spectra, followed by LTQ Orbitrap XL (Thermo Fisher Scientific) spectrometer using ESI technique for high-resolution mass spectra.

For flash chromatography, Teledyne ISCO CombiFlash Rf200 with dual λ absorbance detector and various types of columns were used: a) original Teledyne ISCO columns RediSepRf® variation "HP Silica GOLD" in sizes 12 g, 40 g, 80 g and 120 g; b) original Teledyne ISCO columns RediSepRf® variation "HP C18 Aq GOLD" in sizes 50 g and 100 g; c) column CHROMABOND Flash DL 40, DL 80, DL 120 and DL 200, filled by FLUKA silica gel 60. Separation of UV non-absorbing substances were made: a) with internal UV absorption standard (like caffeine) with similar $R_f$ as required substance; b) by capturing all fractions followed by analysis.

Purity of target compounds was ≥95%. Purity was determined by the combination of UPLC-PDA-MS, NMR and HR-MS.

**UPLC-MS:**

**Procedure 1:** Analytical sample was prepared typically so that 50 µl reaction mixture or chromatographic fraction was diluted in suitable solvent (MeOH or acetonitrile) to concentration about 1 mg of sample in 1 mL of solution. Mixture was diluted to 1-2 mL volume and filtered over syringe filter (0.22 µM, membrane material = PVDF).

Samples were tested by universal LC method (eluent $H_2O/CH_3CN$, gradient 0-100 %, run length 7 min) and time-tested MS method (ESI+, cone voltage = 30V, mass detector range ~ 100-1000 Da in standard case; 500-1600 Da for measurement of prodrugs).

Analytical arrangement contains: Waters UPLC H-Class Core System, (column Waters Acquity UPLC BEH C18 1.7 µm, 2.1x100 mm), Waters Acquity UPLC PDA detector, Mass spectrometer Waters SQD2.

**Procedure 2:** Procedure is almost identical as described above in Procedure 1. There are differences in solvent for dilution of samples (water) and MS method (ESI-, detector range ~ 100-1000 Da). This procedure is suitable for measurement of free phosphonic acids or their sodium salts.

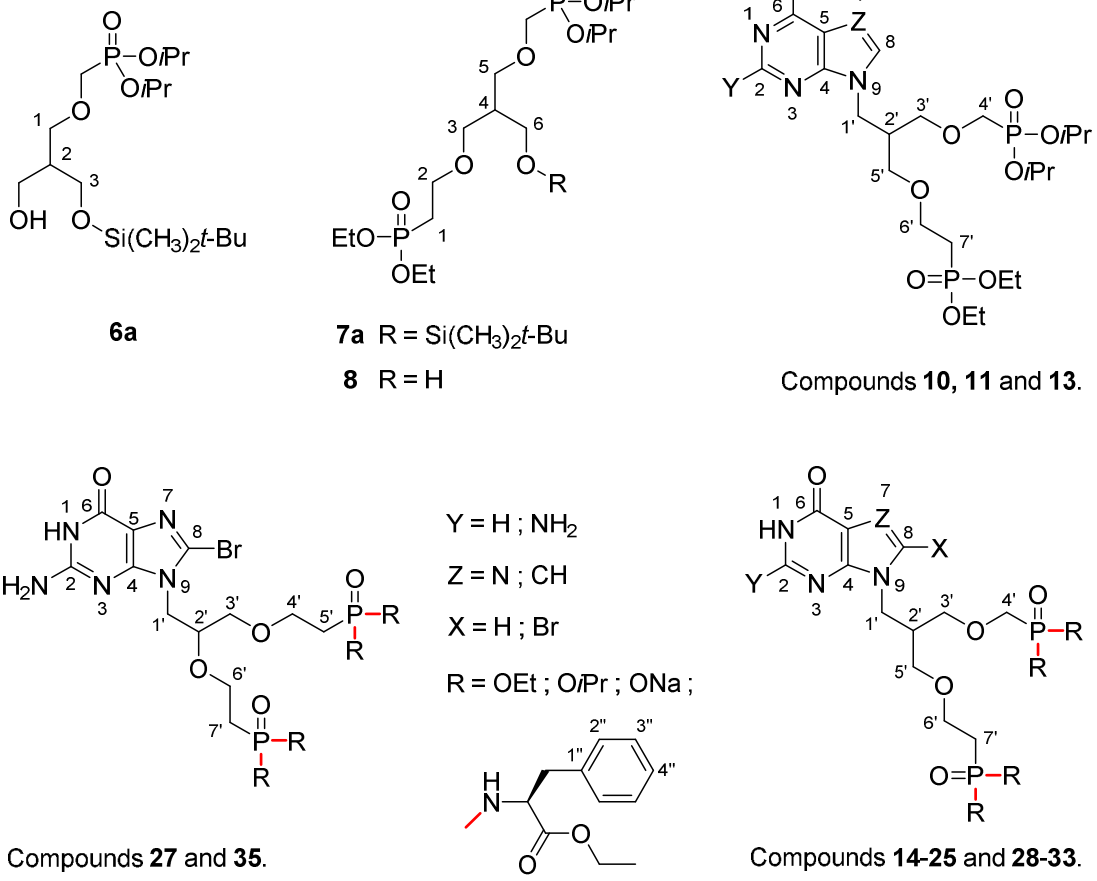


**Figure 11.** Structures and a numbering system for the assignment of NMR signals of compounds in experimental section.

**Synthetic procedures**

General procedure for **Mitsunobu reaction** (**Method A**): To a solution of triphenylphosphine (3.5 g, 13.4 mmol) in dry THF (50 mL) cooled to –30°C under argon atmosphere diisopropyl azadicarboxylate (DIAD, 2.4 mL, 12.2 mmol) was added. The mixture was stirred for 30 min to form a complex. The solution of the corresponding alcohol (4 mmol) in dry THF (30 mL) and 6-chloropurine (1 g, 6.4 mmol = 1.6 eq.) or 6-chloro-7-deazapurine (1 g, 6.4 mmol = 1.6 eq.) was added to the preformed complex and the reaction flask was filled with argon again. The resulting mixture was slowly warmed up to room

temperature and stirred for two days. MeOH (30 mL) was added to dissolve all possible heterogeneous particles. Solvent was evaporated, and the crude mixture was purified by flash chromatography (silica gel; eluent $CHCl_3$/MeOH, gradient 1-10%). The pure product was obtained as a yellowish solid or a foam.

General procedure for the **Mitsunobu reaction** (**Method B**): Starting from 2-amino-6-chloropurine or 2-amino-6-chloro-7-deazapurine and the corresponding alcohol procedure was identical as described above – Method A. Then after the stirring of the reaction mixture for two days, water (30 mL) and MeOH (30 mL) were added and the mixture was heated at 80°C for 30 h. Solvent was evaporated, the residue was codistilled with toluene, and the crude mixture purified by flash chromatography (silica gel; eluent $CHCl_3$/MeOH, gradient 2-15%).

General procedure for **hydrolysis of 6-chloropurine and 2-amino-6-chloropurine derivatives** to corresponding 6-oxopurine and 2-amino-6-oxopurine derivatives (**Method C**): The 6-chloropurine or 2-amino-6-chloropurine derivative (4.13 mmol) was dissolved in aqueous trifluoroacetic acid (75%, 60 mL) and stirred overnight at room temperature. The solvent was evaporated and the residue was codistilled with water (3×) and toluene (2×). The crude product was purified by flash chromatography (silica gel; eluent $CHCl_3$/MeOH, gradient 2-15%). Pure product was obtained as a solidified oil.

General procedure for **hydrolysis of 6-chloro-7-deazapurine and 2-amino-6-chloro-7-deazapurine derivatives** to corresponding 6-oxo-7-deazapurine and 2-amino-6-oxo-7-deazapurine derivatives (**Method D**): The appropriate 6-chloropurine derivative (3 mmol) was dissolved or suspended in water (40 mL) containing $K_2CO_3$ (1.69 g, 12.2 mmol) and DABCO (0.69 g, 6.2 mmol). The reaction mixture was stirred and heated to 120 °C for 1-4 h. The resultant solution was cooled down, neutralized by 1 M HCl and a product extracted to $CHCl_3$ (3x 50 mL). Organic phase was washed with water (2x 100 mL), followed by brine (1x

100 mL) and dried over $MgSO_4$. Compounds were purified by flash chromatography (silica gel; $CHCl_3$/MeOH, gradient 2-10 %). Reaction was monitored by LC-MS (Procedure 1).

General procedure for **synthesis of sodium salts of free bisphosphonates** (**Method E**): A mixture of bisphosphonic acid diester (diisopropyl or diethyl ester) (1 mmol), acetonitrile (20 mL) and $BrSiMe_3$ (2 mL) was stirred overnight at room temperature. After evaporation, the residue was stirred with MeOH:water (1:1, 100 mL) for 2 h at room temperature. The solvent was evaporated *in vacuo*. The residue was dissolved in solution of TEAB (5 mL 2M aqueous TEAB), evaporated *in vacuo* and codistilled with water (3x). That TEAB-salt was purified by flash chromatography (C18 silica gel, 0.125 M aqueous TEAB/MeOH, gradient 0-40%) and evaporated *in vacuo* and codistilled with water (3x). The residue was dissolved in small volume of water (5 mL) and percolated through DOWEX (50WX8 $Na^+$, 5 g) to obtain sodium salt of the bisphosphonic acid. Filtrate was partially evaporated and prepared for following manipulation by lyophilisation from water.

General procedure for **bromination of 6-oxopurine derivatives** (**Method F**): To a solution of corresponding 6-oxopurine derivative (2 mmol) in DMF (10 mL), 0.3 M solution of bromine in $CCl_4$ (13 mL, 4 mmol of $Br_2$, 2 eq.) was added. Reaction mixture was stirred for 2-12 h at room temperature. The mixture was evaporated *in vacuo*, codistilled with toluene (3x) and purified by flash chromatography (silica gel; $CHCl_3$/MeOH, gradient 1-10%). Reaction was monitored by LC-MS (Procedure 1). The product was obtained as colourless/yellowish solidified oil.

General procedure for **synthesis of tetra-(L-phenylalanine ethylester) prodrug of bisphosphonates** (**Method G**): Bisphosphonic acid tetraester (diisopropyl or diethyl ester) (1 mmol) was codistilled with dry acetonitrile (2x). Dry acetonitrile (20 mL) and bromotrimethylsilane (2 mL) were mixed with bisphosphonic acid tetraester and stirred overnight at room temperature under argon. After evaporation *in vacuo* and codistillation with

dry acetonitrile (3x) (without any contact with air), the flask was purged with argon and amino acid ester hydrochloride (2.5 g, 10.88 mmol, dried *in vacuo* at 30°C and 0.1 mbar for 1 day), dry triethylamine (5 mL), and dry pyridine (15 mL) were added and this mixture was stirred and heated to 70 °C. Solution of 2,2'-dipyridyldisulfide (3.4 g, 15.4 mmol) and triphenylphosphine (4 g, 15.4 mmol) in 15 mL of dry pyridine under argon was added immediately. The resulting mixture was heated at 70 °C for 3 days to reach the full conversion. After cooling to room temperature, the richly yellow solution was evaporated *in vacuo* and the residue was purified first by flash chromatography (silica gel; $CHCl_3$/MeOH, gradient 2-15%), followed by flash chromatography again (C18 silica gel, eluent $H_2O$/MeOH, gradient 70-100%). The product was obtained as colourless/yellowish foam and prepared for following manipulation by lyophilisation from dioxan.

General procedure for **bromination of tetra-(L-phenylalanine ethylester) prodrug of bisphosphonates** (**Method H**): The corresponding parent prodrug (0.15 mmol) and NBS (67 mg, 0.38 mmol, 2.5 eq.) were placed into 10 mL MW reactor cuvette and dioxan (6 mL) was added. Cuvette was filled with argon and sealed with a septum. Reaction mixture was stirred in MW reactor at 100 °C for 20 min. The mixture was evaporated and purified first by flash chromatography (silica gel; eluent $CHCl_3$/MeOH, gradient 2-15%), followed by flash chromatography again (C18 silica gel, eluent $H_2O$/MeOH, gradient 70-100%). Compounds were prepared for following manipulation by lyophilisation from dioxan.

**Diisopropyl {[(2,2-dimethyl-1,3-dioxan-5-yl)methoxy]methyl}phosphonate** (**4**)

To the solution of compound **3** (16.1 g, 110 mmol, 1 eq.) in dry DMF (600 mL) cooled to 0°C under argon atmosphere NaH (60% suspension in mineral oil; 7.5 g, 188 mmol, 1.7 eq) was added. Reaction flask was filled with argon again and the mixture was stirred for 20 min to preform sodium salt of alcohol. Diisopropyl (bromomethyl)phosphonate (85% purity; 43.5 g, 143 mmol, 1.3 eq.) was added and reaction flask was filled with argon again. The resulting

mixture was slowly warmed up to room temperature and stirred overnight. Water (50 mL) was added and mixture was stirred for 30 min. Solvent was evaporated *in vacuo*. Crude material was dissolved in EtOAc (250 mL), transferred to separatory funnel. The mixture of saturated solution of $NH_4Cl$ (20 mL) and $H_2O$ (180 mL) was added and organic phase was separated. Aqueous phase was extracted witch EtOAc (2x 150 mL). The organic phase was collected and washed by water (2x 200 mL), followed by brine (1x 200 mL) and dried over $MgSO_4$. The solution was filtered and evaporated *in vacuo*. Crude product was obtained as brown oil and used in the next reaction step without purification. Reaction was monitored by LC-MS (Procedure 1).

MS (ESI+) m/z = 325.2 $[M + H]^+$.

**Diisopropyl {[3-hydroxy-2-(hydroxymethyl)propoxy]methyl}phosphonate (5)**

Crude material of **4** was dissolved in MeOH (500 mL) and $H_2O$ (50 mL). DOWEX (50WX8 $H^+$, 10 g) was added and mixture was heated at 50 °C and stirred overnight. Reaction mixture was cooled down to room temperature and filtered through the frit (S3) and evaporated *in vacuo*. Crude compound was purified by flash chromatography (silica gel; eluent hexane:EtOAc [6:4]/MeOH, gradient 1-10%) to give 12.54 g (the overall yield from compound **3** was 40 %) of **5** as colourless oil.

$^1$H NMR (DMSO-$d_6$): 4.59 [dsept, 2H, $J$(H,C,O,P) = 7.7 Hz, $J$(CH,$CH_3$) = 6.2 Hz, CH *i*Pr]; 4.38 [t, 2H, $J$(OH,$CH_2$) = 5.2 Hz, OH]; 3.68 [d, 2H, $J$(H,C,P) = 8.2 Hz, $CH_2$P]; 3.49 [d, 2H, $J$($CH_2$,CH) = 6.0 Hz, HO-$CH_2$CH$\underline{CH_2}$]; 3.40 [m, 4H, $\underline{CH_2}$-OH]; 1.74 [sept, 1H, $J$(CH,$CH_2$) = 6.0 Hz, OCH$_2\underline{CH}$]; 1.25 and 1.24 [d, 12H, $J$($CH_3$,CH) = 6.2 Hz, $CH_3$ *i*Pr]. $^{13}$C NMR (DMSO-$d_6$): 71.64 [d, $J$(C,O,C,P) = 12.1 Hz, HO-$CH_2$CH$\underline{CH_2}$]; 70.30 [d, $J$(C,O,P) = 6.4 Hz, CH *i*Pr]; 65.25 [d, $J$(C,P) = 164.4 Hz, $CH_2$P]; 59.40 [$CH_2$OH]; 44.45 [OCH$_2\underline{CH}$]; 24.05 and 23.93 [d, $J$(C,C,O,P) = 3.7 Hz, $J$(C,C,O,P) = 4.6 Hz, $CH_3$ *i*Pr]. MS (ESI+) *m/z* = 285.2 $[M + H]^+$.

**Diisopropyl {[3-(*tert*-butyldimethylsilyloxy)-2-(hydroxymethyl)propoxy]methyl}phosphonate (6a)**

To the solution of **5** (2.34 g, 8.2 mmol, 1 eq.) in dry DMF (45 mL), imidazole (0.9 g, 12.3 mmol, 1.5 eq.) and TBDMSCl (1.26 g, 9 mmol, 1.1 eq.) were added. The mixture was stirred overnight at room temperature. Solvent was evaporated *in vacuo* and codistilled with toluene. Crude product was purified by flash chromatography (silica gel; eluent $CHCl_3$/MeOH, gradient 0-8%) to give 3.9 g (41%) of **6a** as colourless oil.

$^1$H NMR (DMSO-$d_6$): 4.54-4.63 [m, 2H, CH *i*Pr]; 4.42 [bs, 1H, OH]; 3.64-3.71 [m, 2H, $CH_2$-P]; 3.58 [d, 2H, *J*(3,2) = 5.8 Hz, H-3]; 3.46-3.52 [m, 2H, H-1]; 3.37-3.43 [m, 2H, $\underline{CH_2}$-OH]; 1.79 [septet, 1H, *J*(2,$CH_2$) = 5.9 Hz, H-2]; 1.24 and 1.24 [d, 12H, *J*($CH_3$,CH) = 6.2 Hz, $CH_3$ *i*Pr]; 0.86 [s, 9H, C-($\underline{CH_3}$)$_3$]; 0.02 [s, 6H, Si-$\underline{CH_3}$]. $^{13}$C NMR (DMSO-$d_6$): 71.27 [d, *J*(1,P) = 12.1 Hz, C-1]; 70.21 [d, *J*(C,O,P) = 6.3 Hz, CH *i*Pr]; 65.32 [d, *J*(C,P) = 164.5 Hz, $CH_2$-P]; 60.94 [C-3]; 59.03 [$\underline{CH_2}$-OH]; 44.39 [C-2]; 25.97 [C-($\underline{CH_3}$)$_3$]; 24.01 and 23.90 [d, *J*(C,C,O,P) = 3.7 Hz, *J*(C,C,O,P) = 4.5 Hz, $CH_3$ *i*Pr]; 18.14 [$\underline{C}$-($CH_3$)$_3$]; -5.30 [Si-$\underline{CH_3}$]. MS (ESI+) *m/z* = 399.05 $[M + H]^+$.

**Diisopropyl{[3-(*tert*-butyldimethylsilyloxy)-2-((2-diethoxyphosphorylethoxy)methyl)propoxy]methyl}phosphonate (7a)**

Alcohol **6a** (7.5 g, 18.8 mmol, 1 eq) and cesium carbonate (6.4 g, 19.7 mmol, 1.05 eq) were placed into 25 mL reaction flask. Dry *tert*-butanol (15 mL) was added, the flask was sealed with a septum and filled with argon. Diethyl vinylphosphonate (5.5 mL, 35.8 mmol, 1.9 eq.) was added into the flask and the mixture was vigorously stirred for two days. The reaction mixture was diluted with $H_2O$ and extracted with EtOAc (3x 100 mL). The organic phase was collected, washed with $H_2O$ (2x 100 mL), followed by brine (1x 100mL) and dried over $MgSO_4$. The solution was filtered and evaporated *in vacuo*. Crude product was obtained as colourless solidified oil and used in the next reaction step without purification. Reaction

was monitored by LC-MS (Procedure 1). Small amount of crude product was purified by flash chromatography (silica gel; eluent hexane/EtOAc [6:4]/MeOH, gradient 1-10%) to obtain an analytical sample.

$^1$H NMR (DMSO-$d_6$): 4.54-4.63 [m, 2H, CH *i*Pr]; 3.93-4.02 [m, 4H, $\underline{CH_2}CH_3$]; 3.65-3.72 [m, 2H, $CH_2$-P]; 3.48-3.61 [m, 6H, H-2, H-5, H-6]; 3.37 [m, 2H, H-3]; 1.99-2.05 [m, 2H, H-1]; 1.93 [m, H-4]; 1.20-1.25 [m, 18H, $CH_3$ *i*Pr, $CH_2\underline{CH_3}$]; 0.86 [s, 9H, $C(CH_3)_3$]; 0.02 [s, 6H, Si-$CH_3$]. $^{13}$C NMR (DMSO-$d_6$): 71.01 [d, *J*(3,P) = 12.0 Hz, C-5]; 70.22 and 70.21 [d, *J*(C,O,P) = 6.4 Hz, CH *i*Pr]; 68.11 [C-3]; 65.28 [d, *J*($CH_2$-P,P) = 164.4 Hz, $CH_2$-P]; 64.74 [d, *J*(2,P) = 1.5 Hz, C-2]; 61.10 [d, *J*(C,O,P) = 6.1 Hz, $\underline{CH_2}CH_3$]; 60.67 [C-6]; 41.93 [C-4]; 26.11 [d, *J*(1,P) = 137.1 Hz, C-1]; 25.94 [$C(\underline{CH_3})_3$]; 24.00 and 23.89 [d, *J*(C,O,O,P) = 3.7 Hz, *J*(C,O,O,P) = 4.5 Hz, $CH_3$ *i*Pr]; 18.11 [$\underline{C}(CH_3)_3$]; 16.42 [d, *J*(C,O,O,P) = 5.9 Hz, $CH_2\underline{CH_3}$]; -5.35 nad -5.36 [Si-$CH_3$]. MS (ESI+) m/z = 563.3 $[M + H]^+$.

**Diisopropyl{[3-hydroxy-2-((2-diethoxyphosphorylethoxy)methyl)propoxy]methyl}phosphonate** (**8**)

Crude product **7a** was dissolved in MeOH:$H_2O$ (100+10 mL). DOWEX (50WX8 $H^+$; 10 g) was added and reaction mixture was heated at 50 °C and stirred overnight. The mixture was filtered and filtrate was evaporated *in vacuo*. Resulting residue was purified by flash chromatography (silica gel; eluent $CHCl_3$/MeOH, gradient 0-10%) to give 5.1 g (overall yield from compound **6a**: 31%) of **8** as colourless oil. Reaction was monitored by LC-MS (Procedure 1) and TLC (eluent $CHCl_3$, 10% MeOH).

$^1$H NMR (DMSO-$d_6$): 4.59 [dsept, 2H, *J*(H,C,O,P) = 7.7 Hz, *J*(CH,$CH_3$) = 6.2 Hz, CH *i*Pr]; 4.47 [t, *J*(OH,$CH_2$) = 5.3 Hz, OH]; 3.94-4.02 [m, 4H, $\underline{CH_2}CH_3$]; 3.69 [d, 2H, *J*(H,C,P) = 8.2 Hz, P-$CH_2$O]; 3.46-3.55 [m, 4H, H-2, H-5]; 3.35-3.41 [m, 4H, H-6, H-3]; 2.03 [dt, 2H, *J*(1,P) = 18.2 Hz, *J*(1,2) = 7.3 Hz, H-1]; 1.87 [sept, 1H, *J*(4,3) = *J*(4,5) = *J*(4,6) = 6.0 Hz, H-4]; 1.21-

1.25 [m, 18H, $CH_3$]. $^{13}C$ NMR (DMSO-$d_6$): 71.38 [d, $J$(5,P) = 12.1 Hz, C-5]; 70.27 [d, $J$(C,O,P) = 6.4 Hz, CH *i*Pr]; 68.52 [C-3]; 65.23 [d, $J$(C,P) = 164.4 Hz, P-$CH_2$O]; 64.67 [d, $J$(2,P) = 1.6 Hz, C-2]; 64.14 [d, $J$(C,O,P) = 6.2 Hz, $\underline{CH_2}CH_3$]; 59.22 [C-6]; 42.12 [C-4]; 26.06 [d, $J$(1,P) = 137.0 Hz, C-1]; 24.03 and 23.92 [d, $J$(C,C,O,P) = 3.8 Hz, $J$(C,C,O,P) = 4.5 Hz, $CH_3$ *i*Pr]; 16.45 [d, $J$(C,C,O,P) = 5.9 Hz, $\underline{CH_3}CH_2$]. MS (ESI+) *m/z* = 449.2 $[M + H]^+$.

**Diisopropyl {[3-(2-amino-6-chloropurin-9-yl)-2-((2-diethoxyphosphorylethoxy)methyl)propoxy]methyl}phosphonate (10)**

From compound **8** (1.55 g, 3.46 mmol) according to **Method B**, afforded 1.53 g (74%) of **10**, as yellowish solid.

$^1H$ NMR (DMSO-$d_6$): 8.10 [s, H-8]; 6.91 [bs, 2H, $NH_2$]; 4.54-4.63 [m, 2H, CH *i*Pr]; 4.07-4.12 [m, 2H, H-1']; 3.93-4.01 [m, 4H, $\underline{CH_2}CH_3$]; 3.68-3.75 [m, 2H, H-4']; 3.44-3.55 [m, 4H, H-3', H-6']; 3.29-3.41 [m, 2H, H-5']; 2.45 [m, 1H, H-2']; 1.97-2.06 [m, 2H, H-7']; 1.20-1.24 [m, 18H, $CH_3$]. $^{13}C$ NMR (DMSO-$d_6$): 159.97 [C-2]; 154.54 [C-4]; 149.47 [C-6]; 143.93 [C-8]; 123.49 [C-5]; 71.12 [d, $J$(3',P) = 11.1 Hz, C-3']; 70.37 and 70.34 [d, $J$(C,O,P) = 6.4 Hz, CH *i*Pr]; 68.38 [C-5']; 65.25 [d, $J$(4',P) = 163.9 Hz, C-4']; 64.70 [C-6']; 61.17-61.24 [m, $\underline{CH_2}CH_3$]; 42.36 [C-1']; 38.92 [C-2']; 25.88 [d, $J$(7',P) = 137.2 Hz, C-7']; 24.00 and 23.91 [d, $J$(C,C,O,P) = 3.7 Hz, $J$(C,C,O,P) = 4.5 Hz, $CH_3$ *i*Pr]; 16.44 [d, $J$(C,C,O,P) = 5.8 Hz, $CH_2\underline{CH_3}$]. MS (ESI+) *m/z* = 600.3 $[M + H]^+$.

**Diisopropyl {[3-(6-chloropurin-9-yl)-2-((2-diethoxyphosphorylethoxy)methyl)propoxy]methyl}phosphonate (11)**

From compound **8** (2.17 g, 4.8 mmol) according to **Method A**, afforded 820 mg (29%) of **11** as colorless solidified oil.

$^1H$ NMR (DMSO-$d_6$): 8.77 [s, 1H, H-2]; 8.70 [s, 1H, H-8]; 4.54-4.63 [m, 2H, CH *i*Pr]; 4.35 [d, 2H, $J$(1',2') = 7.0 Hz, H-1']; 3.92-4.01 [m, 4H, $\underline{CH_2}CH_3$]; 3.68-3.74 [m, 2H, H-4']; 3.50-3.55 [m, 2H, H-3']; 3.42-3.49 [m, 2H, H-6']; 3.33-3.39 [m, 2H, H-5']; 2.52 [m, 1H, H-2'];

1.95 [dt, 2H, $J$(7',P) = 18.2 Hz, $J$(7',6') = 7.2 Hz, H-7']; 1.19-1.24 [m, 18H, $CH_3$]. $^{13}$C NMR (DMSO-$d_6$): 152.45 [C-6]; 151.62 [C-2]; 149.10 [C-4]; 148.24 [C-8]; 131.03 [C-5]; 71.24 [d, $J$(3',P) = 11.3 Hz, C-3']; 70.36 and 70.34 [d, $J$(C,O,P) = 6.4 Hz, CH *i*Pr]; 68.61 [C-5']; 65.21 [d, $J$(4',P) = 164.1 Hz, C-4']; 64.73 [d, $J$(6',P) = 1.6 Hz, C-6']; 61.18 and 61.16 [d, $J$(C,O,P) = 6.2 Hz, $\underline{CH_2}CH_3$]; 43.35 [C-1']; 39.14 [C-2']; 25.84 [d, $J$(7',P) = 137.0 Hz, C-7']; 24.00 and 23.91 [d, $J$(C,C,O,P) = 3.8 Hz, $J$(C,C,O,P) = 4.5 Hz, $CH_3$ *i*Pr]; 16.44 [d, $J$(C,C,O,P) = 5.9 Hz, $CH_2\underline{CH_3}$]. MS (ESI+) $m/z$ = 585.2 $[M + H]^+$.

**Diisopropyl{[3-(2-amino-6-chloro-7-deazapurin-9-yl)-2-((2-diethoxyphosphorylethoxy)methyl)propoxy]methyl}phosphonate** (**12**)

From compound **8** (1.3 g, 2.9 mmol) according to **Method B**, afforded 1.2 g (69%) of **12** as yellowish foam. Presence of product was confirmed by LC-MS (Procedure 1). Pure product was used in the next reaction step without additional characterisation.

MS (ESI) m/z = 599.2 $[M + H]^+$.

**Diisopropyl{[3-(6-chloro-7-deazapurin-9-yl)-2-((2-diethoxyphosphorylethoxy)methyl)propoxy]methyl}phosphonate** (**13**)

From compound **8** (2.63 g, 5.9 mmol) according to **Method A**, afforded 2.83 g (82%) of **13** as yellowish solidified oil.

$^1$H NMR (DMSO-$d_6$): 8.62 [s, 1H, H-2]; 7.79 [d, 1H, $J$(8,7) = 3.6 Hz, H-8]; 6.66 [d, 1H, $J$(7,8) = 3.6 Hz, H-7]; 4.54-4.63 [m, 2H, CH *i*Pr]; 4.30-4.39 [m, 2H, H-1']; 3.93-4.01 [m, 4H, $\underline{CH_2}CH_3$]; 3.66-3.74 [m, 2H, H-4']; 3.43-3.53 [m, 4H, H-3', H-6']; 3.28-3.34 [m, 2H, H-5']; 2.46 [m, 1H, H-2'] ; 1.95-2.04 [m, 2H, H-7']; 1.17-1.24 [m, 18H, $CH_3$]. $^{13}$C NMR (DMSO-$d_6$): 151.05 [C-4]; 150.80 [C-6]; 150.45 [C-2]; 132.29 [C-8]; 116.96 [C-5]; 98.67 [C-7]; 71.20 [d, $J$(3',P) = 11.3 Hz, C-3']; 70.38 and 70.36 [d, $J$(C,O,P) = 6.4 Hz, CH *i*Pr]; 68.52 [C-5']; 65.21 [d, $J$(4',P) = 164.0 Hz, C-4']; 64.81 [d, $J$(6',P) = 1.6 Hz, C-6']; 61.16-61.24 [m, $\underline{CH_2}CH_3$]; 43.98 [C-1']; 39.5 [C-2']; 25.90 [d, $J$(7',P) = 137.2 Hz, C-7']; 24.06 and 23.96 [d,

*J*(C,C,O,P) = 3.7 Hz, *J*(C,C,O,P) = 4.5 Hz, $CH_3$ *i*Pr]; 16.50 [d, *J*(C,C,O,P) = 5.9 Hz, $CH_2\underline{CH_3}$]. MS (ESI+) *m/z* = 584.4 $[M + H]^+$.

**Diisopropyl {[3-(guanine-9-yl)-2-((2-diethoxyphosphorylethoxy)methyl)propoxy]methyl}phosphonate** (**14**)

From compound **10** (1.53 g, 2.55 mmol) according to **Method C**, afforded 1.47 g (99%) of **14** as colorless oil.

$^1$H NMR (DMSO-$d_6$): 10.56 [bs, 1H, H-1]; 7.65 [s, 1H, H-8]; 6.46 [bs, 2H, $NH_2$]; 4.56-4.63 [m, 2H, CH *i*Pr]; 3.92-4.02 [m, 6H, H-1', $\underline{CH_2}CH_3$]; 3.68-3.75 [m, 2H, H-4']; 3.45-3.55 [m, 4H, H-3', H-6']; 3.32 [dd, 1H, *J*(gem) = 9.6 Hz, *J*(5'a,2') = 5.4 Hz, H-5'a]; 3.32 [dd, 1H, *J*(gem) = 9.6 Hz, *J*(5'b,2') = 5.2 Hz, H-5'b]; 2.37 [m, 1H, H-2']; 2.03 [dm, 2H, *J*(7',P) = 18.2 Hz, H-7']; 1.20-1.25 [m, 18H, $CH_3$]. $^{13}$C NMR (DMSO-$d_6$): 157.00 [C-6]; 153.71 [C-2]; 151.57 [C-4]; 138.17 [C-8]; 116.72 [C-5]; 71.03 [d, *J*(3',P) = 11.3 Hz, C-3']; 70.37 and 70.35 [d, *J*(C,O,P) = 6.4 Hz, CH *i*Pr]; 68.20 [C-5']; 65.27 [d, *J*(4',P) = 164.2 Hz, C-4']; 64.71 [d, *J*(6',P) = 1.5 Hz, C-6']; 61.22 and 61.20 [d, *J*(C,O,P) = 6.2 Hz, $\underline{CH_2}CH_3$]; 41.82 [C-1']; 39.27 [C-2']; 25.91 [d, *J*(7',P) = 137.1 Hz, C-7']; 23.91-24.04 [m, $CH_3$ *i*Pr]; 16.45 [d, *J*(C,C,O,P) = 5.9 Hz, $CH_2\underline{CH_3}$]. MS (ESI+) *m/z* = 582.3 $[M + H]^+$.

**Diisopropyl {[3-(hypoxanthine-9-yl)-2-((2-diethoxyphosphorylethoxy)methyl)propoxy]methyl}phosphonate** (**15**)

From compound **11** (820 mg, 1.4 mmol) according to **Method C**, afforded 515 mg (65%) of **15** as yellowish oil.

$^1$H NMR (DMSO-$d_6$): 12.30 [bs, 1H, H-1]; 8.06 [s, 1H, H-8]; 8.02 [s, 1H, H-2]; 4.54-4.64 [m, 2H, CH *i*Pr]; 4.14-4.21 [m, 2H, H-1']; 3.92-4.02 [m, 4H, $\underline{CH_2}CH_3$]; 3.67-3.75 [m, 2H, H-4']; 3.45-3.51 [m, 4H, H-3', H-6']; 3.33 [dd, 1H, *J*(gem) = 9.6 Hz, *J*(5'a,2') = 5.6 Hz, H-5'a]; 3.30 [dd, 1H, *J*(gem) = 9.6 Hz, *J*(5'b,2') = 5.2 Hz, H-5'b]; 2.42 [m, 1H, H-2']; 1.97-2.03 [m, 2H, H-7']; 1.20-1.25 [m, 18H, $CH_3$]. $^{13}$C NMR (DMSO-$d_6$): 156.91 [C-6]; 148.81 [C-4];

145.68 [C-2]; 141.07 [C-8]; 124.13 [C-5]; 71.11 [d, *J*(3',P) = 11.2 Hz, C-3']; 70.42 and 70.40 [d, *J*(C,O,P) = 6.4 Hz, *J*(C,O,P) = 6.3 Hz, CH *i*Pr]; 68.41 [C-5']; 65.23 [d, *J*(4',P) = 164.0 Hz, C-4']; 64.79 [d, *J*(6',P) = 1.6 Hz, C-6']; 61.23 and 61.21 [d, *J*(C,O,P) = 6.2 Hz, $\underline{CH_2}$-$CH_3$]; 42.63 [C-1']; 39.59 [C-2']; 25.90 [d, *J*(7',P) = 137.1 Hz, C-7']; 24.04 and 23.95 [d, *J*(C,C,O,P) = 3.7 Hz, *J*(C,C,O,P) = 4.5 Hz, $CH_3$ iPr]; 16.47 [d, *J*(C,C,O,P) = 5.9 Hz, $CH_2$-$\underline{CH_3}$]. MS (ESI+) *m/z* = 567.3 $[M + H]^+$.

**Diisopropyl {[3-(8-bromoguanine-9-yl)-2-((2-diethoxyphosphorylethoxy)methyl)propoxy]methyl}phosphonate (16)**

From compound **98** (656 mg, 1.1 mmol) according to **Method F**, afforded 325 mg (45%) of **102** as yellowish-orange oil.

$^1$H NMR (DMSO-$d_6$): 10.67 [s, 1H, H-1]; 6.58 [bs, 2H, $NH_2$]; 4.54-4.63 [m, 2H, CH *i*Pr]; 3.87-4.05 [m, 6H, H-1', $\underline{CH_2}CH_3$]; 3.75 and 3.68 [dd, 2H, *J*(gem) = 14.0 Hz, *J*(4',P) = 8.0, *J*(gem) = 14.0 Hz, *J*(4',P) = 7.8, H-4']; 3.32-3.60 [m, 6H, H-3', H-5', H-6']; 2.43 [m, 1H, H-2']; 1.95-2.05 [m, 2H, H-7']; 1.19-1.25 [m, 18H, $CH_3$]. $^{13}$C NMR (DMSO-$d_6$): 155.78 and 154.00 [C-2, C-6]; 152.94 [C-4]; 121.25 [C-8]; 116.97 [C-5]; 71.11 [d, *J*(3',P) = 10.8 Hz, C-3']; 70.36, 70.34 [d, *J*(C,O,P) = 6.4 Hz, CH *i*Pr]; 68.51 [C-5']; 65.27 [d, *J*(4',P) = 163.8 Hz, C-4']; 64.64 [C-6']; 61.17-61.27 [m, $\underline{CH_2}CH_3$]; 43.30 [C-1']; 39.02 [C-2']; 25.91 [d, *J*(7',P) = 137.0 Hz, C-7']; 23.92-24.05 [m, $CH_3$ *i*Pr]; 16.47 [d, *J*(C,C,O,P) = 5.9 Hz, $CH_2\underline{CH_3}$]. MS (ESI+) *m/z* = 660.4 $[M + H]^+$.

**Diisopropyl {[3-(8-bromohypoxanthine-9-yl)-2-((2-diethoxyphosphorylethoxy)methyl)propoxy]methyl}phosphonate (17)**

From compound **99** (499 mg, 0.89 mmol) according to **Method F**, afforded 155 mg (27%) of **103** as yellowish orange oil.

$^1$H NMR (DMSO-$d_6$): 12.46 [bs, 1H, H-1]; 8.05 [d, 1H, *J*(2,1) = 3.0 Hz, H-2]; 4.53-4.62 [m, 2H, CH*i*Pr]; 4.13-4.21 [m, 2H, H-1']; 3.87-4.00 [m, 4H, $\underline{CH_2}CH_3$]; 3.65-3.75 [m, 2H, H-4'];

3.36-3.57 [m, 6H, H-3', H-5', H-6']; 2.47 [m, 1H, H-2']; 1.90-2.00 [m, 2H, H-7']; 1.18-1.24 [m, 18H, $CH_3$]. $^{13}$C NMR (DMSO-$d_6$): 155.56 [C-6]; 150.26 [C-4]; 146.34 [C-2] ; 125.79 [C-8]; 124.45 [C-5]; 71.19 [d, $J$(3',P) = 11.0 Hz, C-3']; 70.35 [d, $J$(C,O,P) = 6.4 Hz, CH *i*Pr]; 68.76 [C-5']; 65.23 [d, $J$(4',P) = 163.9 Hz, C-4']; 64.73 [C-6']; 61.15-61.20 [m, $\underline{CH_2}CH_3$]; 44.29 [C-1']; 39.0 [C-2']; 25.90 [d, $J$(7',P) = 137.0 Hz, C-7']; 23.92-24.05 [m, $CH_3$ *i*Pr]; 16.46 [d, $J$(C,C,O,P) = 5.9 Hz, $CH_2\underline{CH_3}$]. MS (ESI+) m/z = 645.2 $[M + H]^+$.

**Diisopropyl {[3-(7-deazaguanine-9-yl)-2-((2-diethoxyphosphorylethoxy)methyl)propoxy]methyl}phosphonate** (**18**)

From compound **12** (1139 mg, 1.9 mmol) according to **Method D**, afforded 256 mg (23%) of **18** as colourless oil.

$^1$H NMR (DMSO-$d_6$): 10.28 [bs, 1H, H-1]; 6.71 [d, 1H, $J$(8,7) = 3.4 Hz, H-8]; 6.22 [bs, 2H, $NH_2$]; 6.21 [d, 1H, $J$(7,8) = 3.4 Hz, H-7]; 4.56-4.63 [m, 2H, CH *i*Pr]; 3.87-4.01 [m, 6H, H-1', $\underline{CH_2}CH_3$]; 3.66-3.74 [m, 2H, H-4']; 3.42-3.58 [m, 4H, H-3', H-6']; 3.24-3.30 [m, 2H, H-5']; 2.32 [m, 1H, H-2']; 2.01-2.09 [m, 2H, H-7']; 1.20-1.25 [m, 18H, $CH_3$]. $^{13}$C NMR (DMSO-$d_6$): 158.90 [C-6]; 152.57 [C-2]; 150.61 [C-4]; 120.98 [C-8]; 101.36 [C-7]; 100.07 [C-5]; 71.13 [d, $J$(3',P) = 11.3 Hz, C-3']; 70.38 d and 70.35 [d, $J$(C,O,P) = 6.4 Hz, CH *i*Pr]; 68.26 [C-5']; 65.27 [d, $J$(4',P) = 164.0 Hz, C-4']; 64.72 [C-6']; 61.20-61.27 [m, $\underline{CH_2}CH_3$]; 42.94 [C-1']; 39.7 [C-2']; 23.96-24.09 [m, $CH_3$ *i*Pr]; 16.51 [d, $J$(C,C,O,P) = 5.9 Hz, $CH_2\underline{CH_3}$]. MS (ESI+) *m/z* = 581.3 $[M + H]^+$.

**Diisopropyl{[3-(7-deazahypoxanthine-9-yl)-2-((2-diethoxyphosphorylethoxy)methyl)propoxy]methyl}phosphonate** (**19**)

From compound **13** (2.83 g, 4.85 mmol) according to **Method D**, afforded 1.19 g (43%) of **19** as white solid.

$^1$H NMR (DMSO-$d_6$): 11.90 [bs, 1H, H-1]; 7.87 [s, 1H, H-2]; 7.14 [d, $J$(8,7) = 3.4 Hz, H-8]; 6.46 [d, $J$(7,8) = 3.4 Hz, H-7]; 4.54-4.64 [m, 2H, CH *i*Pr]; 4.13-4.16 [m, 2H, H-1']; 3.93-4.02 [m, 4H, $\underline{CH_2}CH_3$]; 3.68-3.78 [m, 2H, H-4']; 3.42-3.51 [m, 4H, H-3', H-6']; 3.26-3.32 [m, 2H, H-5']; 2.37 [m, 1H, H-2']; 1.99-2.07 [m, 2H, H-7']; 1.20-1.25 [m, 18H, $CH_3$]. $^{13}$C NMR (DMSO-$d_6$): 158.48 [C-6]; 147.50 [C-4]; 143.56 [C-2]; 124.57 [C-8]; 107.99 [C-5]; 101.66 [C-7]; 71.15 [d, $J$(3',P) = 11.3 Hz, C-3']; 70.37 and 70.35 [d, $J$(C,O,P) = 6.3 Hz, $J$(C,O,P) = 6.4 Hz, CH *i*Pr]; 68.38 [C-5']; 65.23 [d, $J$(4',P) = 164.1 Hz, C-4']; 64.82 [d, $J$(6',P) = 1.6 Hz, C-6']; 61.16-61.23 [m, $\underline{CH_2}CH_3$]; 43.26 [C-1']; 40.30 [C-2']; 25.94 [d, $J$(7',P) = 137.0 Hz, H-7']; 24.06 and 23.96 [d, $J$(C,O,O,P) = 3.6 Hz, $J$(C,O,O,P) = 4.5 Hz, $CH_3$ *i*Pr]; 16.49 [d, $J$(C,O,O,P) = 5.9 Hz, $CH_2\underline{CH_3}$]. MS (ESI+) m/z = 566.3 $[M + H]^+$.

**Sodium salt of {[3-(guanine-9-yl)-2-((2-phosphonoethoxy)methyl)propoxy]methyl}phosphonic acid** (**20**)

From compound **14** (597 mg, 1.02 mmol) according to **Method E**, afforded 160 mg (30%) of **20** as yellowish lyophilisate.

$^1$H NMR ($D_2O$): 7.83 [s, 1H, H-8]; 4.09-4.19 [m, 2H, H-1']; 3.58-3.67 [m, 4H, H-4', H-6']; 3.53 [d, 2H, $J$(3',2') = 5.8 Hz, H-3']; 3.45-3.51 [m, 2H, H-5']; 2.46 [m, 1H, H-2']; 1.85-1.92 [m, 2H, H-7']. $^{13}$C NMR ($D_2O$): 159.17 [C-6]; 154.19 [C-2]; 152.21 [C-4]; 141.12 [C-8]; 115.93 [C-5]; 71.59 [d, $J$(3',P) = 12.2 Hz, H-3']; 69.40 [C-5']; 67.80 [d, $J$(4',P) = 156.7 Hz, C-4']; 67.04 [C-6']; 43.22 [C-1']; 39.56 [C-2']; 29.34 [d, $J$(7',P) = 130.0 Hz, C-7']. HR-MS (ESI-) *m/z*: calcd for $C_{12}H_{17}N_5Na_4O_9P_2$ 440.07417 $[M - 4\ Na + 3\ H]^-$, found 440.07349 $[M - 4\ Na + 3\ H]^-$.

**Sodium salt of {[3-(hypoxanthine-9-yl)-2-((2-phosphonoethoxy)methyl)propoxy]methyl}phosphonic acid** (**21**)

From compound **15** (84 mg, 0.15 mmol) according to **Method E**, afforded 30 mg (39%) of **21** as yellowish lyophilisate.

$^1$H NMR ($D_2O$): 8.20 [s, H-2]; 8.18 [s, H-8]; 4.35-4.45 [m, 2H, H-1']; 3.49-3.63 [m, 8H, H-3', H-4', H-5', H-6']; 2.56 [m, H-2']; 1.77-1.84 [m, 2H, H-7']. $^{13}$C NMR ($D_2O$): 159.30 [C-6]; 149.87 [C-4]; 146.23 [C-2]; 143.59 [C-8]; 123.82 [C-5]; 71.59 [d, *J*(3',P) = 12.0 Hz, C-3']; 69.56 [C-5']; 67.90 [d, *J*(4',P) = 156.6 Hz, C-4']; 67.15 [d, *J*(6',P) = 1.7 Hz, C-6']; 43.99 [C-1']; 39.87 [C-2']; 29.32 [d, *J*(7',P) = 129.7 Hz, C-7']. HR-MS (ESI-) *m/z*: calcd for $C_{12}H_{16}N_4Na_4O_9P_2$ 425.06327 $[M - 4\ Na + 3\ H]^-$, found 425.06244 $[M - 4\ Na + 3\ H]^-$.

**Sodium salt of {[3-(8-bromoguanine-9-yl)-2-((2-phosphonoethoxy)methyl)propoxy]methyl}phosphonic acid** (**22**)

From compound **16** (294 mg, 0.45 mmol) according to **Method E**, afforded 27 mg (10%) of **22** as white lyophilisate.

$^1$H NMR ($D_2O$): 4.13-4.21 [m, 2H, H-1']; 3.50-3.67 [m, 8H, H-3', H-4', H-5', H-6']; 2.58 [m, 1H, H-2']; 1.71-1.85 [m, 2H, H-7']. $^{13}$C NMR ($D_2O$): 158.41 [C-6]; 154.33 [C-2]; 153.66 [C-4]; 125.76 [C-8]; 116.88 [C-5]; 71.94 [d, *J*(3',P) = 11.7 Hz, C-3']; 70.08 [C-5']; 67.25-68.57 [m, C-4']; 67.13 [C-6']; 44.78 [C-1']; 38.92 [C-2']; 29.38 [d, *J*(7',P) = 129.6 Hz, C-7']. HR-MS (ESI-) *m/z*: calcd for $C_{12}H_{16}BrN_5Na_4O_9P_2$ 517.98469 $[M - 4\ Na + 3\ H]^-$, found 517.98420 $[M - 4\ Na + 3\ H]^-$.

**Sodium salt of {[3-(8-bromohypoxanthine-9-yl)-2-((2-phosphonoethoxy)methyl)propoxy]methyl}phosphonic acid** (**23**)

From compound **17** (135 mg, 0.21 mmol) according to **Method E**, afforded 37 mg (31%) of **23** as yellowish lyophilisate.

$^1$H NMR ($D_2O$): 8.19 [s, 1H, H-2]; 4.35-4.43 [m, 2H, H-1']; 3.45-3.67 [m, 8H, H-3', H-4', H-5', H-6']; 2.64 [m, 1H, H-2']; 1.61-1.77 [m, 2H, H-7']. $^{13}$C NMR ($D_2O$): 158.07 [C-6]; 151.14 [C-4]; 146.61 [C-2]; 129.42 [C-8]; 124.35 [C-5]; 71.92 [d, *J*(3',P) = 11.5 Hz, C-3']; 70.22 [C-5']; 68.43 [d, *J*(4',P) = 154.9 Hz, C-4']; 67.46 [d, *J*(6',P) = 2.6 Hz, C-6']; 45.78 [C-

1']; 39.19 [C-2']; 29.55 [d, *J*(7',P) = 128.6 Hz, C-7']. HR-MS (ESI-) *m/z*: calcd for $C_{12}H_{15}BrN_4Na_4O_9P_2$ 502.97379 [M – 4 Na + 3 H]$^-$, found 502.97318 [M – 4 Na + 3 H]$^-$.

**Sodium salt of {[3-(7-deazaguanine-9-yl)-2-((2-phosphonoethoxy)methyl)propoxy]methyl}phosphonic acid (24)**

From compound **18** (110 mg, 0.19 mmol) according to **Method E**, afforded 29 mg (35%) of **24** as yellowish lyophilisate.

$^1$H NMR ($D_2O$): 6,89 [d, 1H, *J*(8,7) = 3.6 Hz, H-8]; 6.48 [d, 1H, *J*(7,8) = 3.6Hz, H-7]; 4.08-4.16 [m, 2H, H-1']; 3.54-3.64 [m, 4H, H-4', H-6']; 3.52 [m, 2H, H-3']; 3.47 [m, 2H, H-5']; 2.45 [m, 1H, H-2']; 1.83-1.89 [m, 2H, H-7']. $^{13}$C NMR ($D_2O$): 162.11 [C-6]; 152.87 [C-2]; 151.49 [C-4]; 124.46 [C-8]; 101.38 [H-7]; 100.44 [H-5]; 71.83 [d, *J*(3',P) = 12.1 Hz, H-3']; 69.50 [C-5']; 68.0 [C-4']; 67.2 [C-6']; 44.09 [C-1']; 40.16 [C-2']; 29.45 [m, C-7']. HR-MS (ESI-) *m/z*: calcd for $C_{13}H_{18}N_4Na_4O_9P_2$ 461.06087 [M – 3 Na + 2 H]$^-$, found 461.06025 [M – 3 Na + 2 H]$^-$.

**Sodium salt of {[3-(7-deazahypoxanthine-9-yl)-2-((2-phosphonoethoxy)methyl)propoxy]methyl}phosphonic acid (25)**

From compound **19** (649 mg, 1.15 mmol) according to **Method E**, afforded 38 mg (6%) of **25** as yellowish lyophilisate.

$^1$H NMR ($D_2O$): 8.05 [s, 1H, H-2]; 7.22 [d, 1H, *J*(8,7) = 3.5 Hz, H-8]; 6.68 [d, 1H, *J*(7.8) = 3.5 Hz, H-7]; 4.26-4.34 [m, 2H, H-1']; 3.51-3.61 [m, 6H, H-3', H-4', H-6']; 3.43-3.49 [m, 2H, H-5']; 2.49 [m, 1H, H-2']; 1.77-1.87 [m, 2H, H-7']. $^{13}$C NMR ($D_2O$): 161.46 [C-6]; 148.46 [C-4]; 143.47 [C-2]; 127.22 [C-8]; 108.08 [C-5]; 102.01 [C-7]; 71.81 [d, *J*(3',P) = 11.4 Hz, C-3']; 69.51 [C-5']; 67.88 [m, C-4']; 67.12 [C-6']; 44.74 [C-1']; 40.41 [C-2']; 29.31 [d, *J*(7',P) = 129.6 Hz, C-7']. HR-MS (ESI-) *m/z*: calcd for $C_{13}H_{17}N_3Na_4O_9P_2$ 424.06803 [M – 4 Na + 3 H]$^-$, found 424.06732 [M – 4 Na + 3 H]$^-$.

**Diethyl{2-[3-(8-bromoguanine-9-yl)-2-(2-(diethoxyphosphoryl)ethoxy)propoxy]ethyl} phosphonate** (**26**)

From compound **2c** (1.3 g, 2.35 mmol) according to **Method F**, afforded 1.2 g (81%) of **26** as yellowish-orange solidified oil. Presence of product was confirmed by LC-MS (Procedure 1). Pure product was used in the next reaction step without additional characterisation.

HR-MS (ESI+) *m/z*: calcd for $C_{20}H_{36}BrN_5O_9P_2$ 632.12444 $[M + H]^+$, found 632.12445 $[M + H]^+$.

**{2-[3-(8-Bromoguanin-9-yl)-2-(2-(bishydroxyphosphoryl)ethoxy)propoxy]ethyl}phosphonic acid** (**27**)

From compound **26** (1.1 g, 1.74 mmol) according to **Method E**, afforded 434 mg (41%) of **27** as white lyophilisate.

$^1$H NMR ($D_2O$): 4.25 [dd, 1H, *J*(gem) = 15.0 Hz, *J*(1'a,2') = 5.1 Hz, H-1'a]; 4.19 [dd, 1H, *J*(gem) = 15.0 Hz, *J*(1'b,2') = 7.1 Hz, H-1'b]; 3.99 [m, 1H, H-2']; 3.70-3.79 [m, 4H, H-3'a, H-6'a, H-4']; 3.64 [m, 1H, H-6'b]; 3.55 [dd, 1H, *J*(gem) = 10.9 Hz, *J*(3'b,2') = 4.9 Hz, H-3'b]; 1.94-2.00 [m, 2H, H-5']; 1.69-1.83 [m, 2H, H-7']. $^{13}$C NMR ($D_2O$): 158.48 [C-6]; 154.47 [C-2]; 153.73 [C-4]; 125.80 [C-8]; 116.97 [C-5]; 76.61 [C-2']; 70.07 [C-3']; 67.63 [d, *J*(4',P) = 1.6 Hz, C-4']; 66.94 [d, *J*(6',P) = 3.0 Hz, C-6']; 45.54 [C-1']; 29.75 [d, *J*(7',P) = 128.7 Hz, H-7']; 29.49 [d, *J*(5',P) = 129.7 Hz, C-5']. HR-MS (ESI-) *m/z*: calcd for $C_{12}H_{16}BrN_5Na_4O_9P_2$ 517.98469 $[M - 4\ Na + 3\ H]^-$, found 517.98401 $[M - 4\ Na + 3\ H]^-$.

**Tetra-(L-phenylalanine ethylester) prodrug of {[3-(guanine-9-yl)-2-((2-phosphonoethoxy)methyl)propoxy]methyl}phosphonic acid** (**28**)

From compound **14** (608 mg, 1.05 mmol) according to method to **Method G**, afforded 274 mg (62%) of **28** as brilliantly white lyophilisate.

$^1$H NMR (DMSO-$d_6$): 10.57 [bs, H-1]; 7.59 and 7.57 [s, 1 H, H-8]; 7.09-7.27 [m, 20H, H-2'', H-3'', H-4'']; 6.54 [bs, 2H, $NH_2$]; 4.47-4.58 and 4.12-4.25 [m, 4H, NH-CH]; 3.82-4.05 [m, 14H, H-1', NH-CH, $CH_2CH_3$]; 3.08-3.32 [m, 8H, H-3', H-4', H-5', H-6']; 2.70-2.93 [m, 8H, 1''-$CH_2$]; 2.16 [m, H-2']; 1.55 [m, 2H, H-7']; 1.03-1.13 [m, 12H, $CH_3$]. $^{13}$C NMR (DMSO-$d_6$): 172.88-173.37 [m, COO]; 157.07 [C-6]; 153.78 [C-2]; 151.67 and 151.63 [C-4]; 138.35 and 138.31 [C-8]; 137.24-137.52 [m, C-1'']; 129.63-129.71 [m, C-2'']; 128.31-128.37 [m, C-3'']; 126.67-126.76 [m, C-4'']; 116.65 [C-5]; 70.55-70.75 [m, C-3']; 67.28-68.43 [m, C-4', C-5']; 65.08 and 65.02 [C-6']; 60.53-60.72 [m, $CH_2CH_3$]; 53.98-54.49 [m, CH-NH]; 41.25 [C-1']; 39.9 [1''-$CH_2$]; 39.1 [C-2']; 30.14 [d, $J$(7',P) = 111.9 Hz, C-7']; 14.10-14.18 [m, $CH_3$]. HR-MS (ESI+) *m/z*: calcd for $C_{56}H_{73}N_9O_{13}P_2$ 1164.46953 $[M + Na]^+$, found 1164.47004 $[M + Na]^+$.

**Tetra-(L-phenylalanine ethylester) prodrug of {[3-(hypoxanthine-9-yl)-2-((2-phosphonoethoxy)methyl)propoxy]methyl}phosphonic acid** (**29**)

From compound **15** (888 mg, 1.6 mmol) according to **Method G**, afforded 449 mg (25%) of **29** as white lyophilisate.

$^1$H NMR (DMSO-$d_6$): 12.32 [bs, H-1]; 8.02 and 8.00 [s, 1H, H-2]; 7.99 and 7.96 [s, 1H, H-8]; 7.11-7.27 [m, 20H, H-2'', H-3'', H-4'']; 4.46-4.64 [m, 2H, NH-CH]; 4.24 [m, 1H, NH-CH]; 3.82-4.12 [m, 15H, NH-CH, NH-CH, $CH_2CH_3$, H-1']; 2.99-3.28 [m, 8H, H-3', H-4', H-5', H-6']; 2.69-2.94 [m, 8H, 1''-$CH_2$]; 2.09-2.25 [m, 1H, H-2']; 1.48-1.57 [m, 2H, H-7']; 1.04-1.15 [m, 12H, $CH_3$]. $^{13}$C NMR (DMSO-$d_6$): 172.96-173.41 [m, COO]; 156.92 and 156.90 [C-6]; 148.78 and 148.69 [C-4]; 145.80 and 145.73 [C-2]; 141.23 and 141.06 [C-8]; 137.30-137.52 [m, C-1'']; 129.68-129.72 [m, C-2'']; 128.31-128.36 [m, C-3'']; 126.66-126.74 [m, C-4'']; 124.04 and 124.01 [C-5]; 70.21-70.63 [m, C-3']; 67.11-68.59 [m, C-4', C-5']; 65.36 [C-6']; 60.53-60.73 [m, $CH_2CH_3$]; 53.86-54.45 [m, CH-NH]; 42.00 and 41.89 [C-1']; 39.7 [1''-$CH_2$];

39.4 [C-2']; 30.00 [d, *J*(7',P) = 112.3 Hz, C-7']; 14.12-14.20 [m, $CH_3$]. HR-MS (ESI+) *m/z*: calcd for $C_{56}H_{72}N_8O_{13}P_2$ 1127.47668 $[M + H]^+$, found 1127.47724 $[M + H]^+$.

**Tetra-(L-phenylalanine ethylester) prodrug of {[3-(7-deazaguanine-9-yl)-2-((2-phosphonoethoxy)methyl)propoxy]methyl}phosphonic acid (30)**

From compound **18** (110 mg, 0.19 mmol) according to **Method G**, afforded 49 mg (23%) of **30** as white lyophilisate.

$^1$H NMR (DMSO-$d_6$): 10.32 [bs, 1H, H-1]; 7.08-7.27 [m, 20H, H-2'', H-3'', H-4'']; 6.61 and 6.60 [d, 1H, *J*(8,7) = 3.4 Hz, H-8]; 6.30 [bs, 2H, $NH_2$]; 6.22 and 6.21 [d, 1H, *J*(7,8) = 3.4 Hz, H-7]; 4.42-4.56 and 4.09-4.21 [m, 4H, NH]; 3.78-4.04 [m, 14H, H-1', NH-CH, $CH_2CH_3$]; 3.07-3.35 [m, 8H, H-3', H-4', H-5', H-6']; 2.70-2.93 [m, 8H, 1''-$CH_2$]; 2.14 [m, 1H, H-2']; 1.51-1.60 [m, 2H, H-7']; 1.03-1.13 [m, 12H, $CH_3$]. $^{13}$C NMR (DMSO-$d_6$): 172.81-173.33 [m, COO]; 158.93 [C-6]; 152.59 [C-2]; 150.65 and 150.63 [C-4]; 137.18-137.50 [m, C-1'']; 129.59-129.68 [m, C-2'']; 128.29-128.34 [m, C-3'']; 126.65-126.73 [m, C-4'']; 121.07 and 121.03 [C-8]; 101.27 [C-7]; 99.98 [C-5]; 70.87-71.06 [m, C-3']; 67.35-68.50 [m, C-4', C-5']; 65.07 and 65.01 [C-6']; 60.49-60.70 [m, $CH_2CH_3$]; 53.99-54.47 [m, NH-CH]; 42.59 [C-1']; 39.8 [1''-$CH_2$]; 39.6 [C-2']; 30.15 [d, *J*(7',P) = 113.7 Hz, C-7']; 14.08-14.16 [m, $CH_3$]. HR-MS (ESI+) *m/z*: calcd for $C_{57}H_{74}N_8O_{13}P_2$ 1163.47428 $[M + Na]^+$, found 1163.47445 $[M + Na]^+$.

**Tetra-(L-phenylalanine ethylester) prodrug of {[3-(7-deazahypoxanthine-9-yl)-2-((2-phosphonoethoxy)methyl)propoxy]methyl}phosphonic acid (31)**

From compound **19** (508 mg, 0.9 mmol) according to **Method G**, afforded 108 mg (11%) of **31** as white lyophilisate.

$^1$H NMR (DMSO-$d_6$): 11.92 [bs, 1H, H-1]; 7.90 and 7.87 [s, 1H, H-2]; 7.10-7.27 [m, 20H, H-2'', H-3'', H-4'']; 7.03 and 7.00 [d, 1H, *J*(8,7) = 3.4 Hz, H-8]; 6.48 and 6.47 [d, 1H, *J*(7,8) = 3.4 Hz, H-7]; 4.46-4.62 [m, 2H, NH]; 4.20 [m, 1H, NH]; 3.81-4.12 [m, 15H, NH, NH-CH,

$\underline{CH_2}CH_3$, H-1']; 2.98-3.32 [m, 8H, H-3', H-4', H-5', H-6']; 2.69-2.94 [m, 8H, 1''-$\underline{CH_2}$]; 2.19 and 2.10 [m, 1H, H-2']; 1.48-1.59 [m, 2H, H-7']; 1.04-1.14 [m, 12H, $CH_3$]. $^{13}$C NMR (DMSO-$d_6$): 173.12-173.60 [m, COO]; 158.72 and 158.70 [C-6]; 147.72 and 147.64 [C-4]; 143.93 and 143.83 [C-2]; 137.52-137.74 [m, C-1'']; 129.87-129.94 [m, C-2'']; 128.53-128.57 [m, C-3'']; 126.89-126.96 [m, C-4'']; 124.91 and 124.71 [C-8]; 108.15 and 108.10 [C-5]; 101.97 and 101.89 [C-7]; 71.09 and 70.72 [d, $J$(3',P) = 13.0 Hz, $J$(3',P) = 13.5 Hz, C-3']; 67.42-68.91 [m, C-4', C-5']; 65.56 [C-6']; 60.74-60.95 [m, $\underline{CH_2}CH_3$]; 54.14-54.67 [m, $\underline{CH}$-NH]; 43.46 and 43.33 [C-1']; 39.8 [1''-$\underline{CH_2}$]; 29.84-30.77 [m, C-7']; 14.34-14.42 [m, $CH_3$]. HR-MS (ESI+) *m/z*: calcd for $C_{57}H_{73}N_7O_{13}P_2$ 1148.46338 $[M + Na]^+$, found 1148.46358 $[M + Na]^+$.

**Tetra-(L-phenylalanine ethylester) prodrug of {[3-(8-bromoguanine-9-yl)-2-((2-phosphonoethoxy)methyl)propoxy]methyl}phosphonic acid (32)**

From compound **28** (160 mg, 0.14 mmol) according to **Method H**, afforded 21 mg (12%) of **32** as colourless oil.

$^1$H NMR (DMSO-$d_6$): 10.73 [bs, 1H, H-1]; 7.06-7.27 [m, 20H, H-2'', H-3'', H4'']; 6.73 [bs, 2H, $NH_2$]; 4.08-4.61 [m, 4H, NH]; 3.79-4.05 [m, 12H, NH-$\underline{CH}$, $\underline{CH_2}CH_3$]; 3.08-3.38 [m, 8H, H-3', H-4', H-5', H-6']; 2.67-2.93 [m, 8H, 1''-$\underline{CH_2}$]; 2.23 [m, 1H, H-2']; 1.50-1.60 [m, 2H, H-7']; 1.01-1.14 [m, 12H, $CH_3$]. $^{13}$C NMR (DMSO-$d_6$): 172.78-173.36 [m, COO]; 155.85 and 154.13 [C-2, C-6]; 152.93 [C-4]; 137.17-137.55 [m, C-1'']; 129.56-129.69 [m, C-2'']; 128.26-128.35 [m, C-3'']; 126.61-126.75 [m, C-4'']; 121.21 and 121.19 [C-8]; 116.89 [C-5]; 70.86-71.03 [m, C-3']; 67.38-68.43 [m, C-4', C-5']; 65.01 and 64.89 [C-6']; 60.47-60.75 [m, $\underline{CH_2}CH_3$]; 53.94-54.54 [m, $\underline{CH}$-NH]; 42.54 and 42.45 [C-1']; 39.8 [1''-$\underline{CH_2}$]; 38.7 [C-2']; 29.8 [C-7']; 14.50-14.17 [m, $CH_3$]. HR-MS (ESI+) *m/z*: calcd for $C_{56}H_{72}BrN_9O_{13}P_2$ 1220.39810 $[M + H]^+$, found 1220.39888 $[M + H]^+$.

**Tetra-(L-phenylalanine ethylester) prodrug of {[3-(8-bromohypoxanthine-9-yl)-2-((2-phosphonoethoxy)methyl)propoxy]methyl}phosphonic acid (33)**

From compound **29** (153 mg, 0.136 mmol) according to **Method H**, afforded 24 mg (15%) of **33** as white lyophilisate.

$^1$H NMR (DMSO-$d_6$): 12.49 [bs, 1H, H-1]; 8.05, 8.01 [s, 1H, H-2]; 7.09-7.27 [m, 20H, H-2'', H-3'', H-4'']; 4.14-4.59 [m, 4H, NH]; 3.80-4.11 [m, 14H, H-1', NH-CH, $CH_2CH_3$]; 3.07-3.33 [m, 8H, H-3', H-4', H-5', H-6']; 2.67-2.92 [m, 8H, 1''-$CH_2$]; 2.21-2.32 [m, 1H, H-2']; 1.43-1.56 [m, 2H, H-7']; 1.03-1.17 [m, 12H, $CH_3$]. $^{13}$C NMR (DMSO-$d_6$): 172.91-173.30 [m, COO]; 155.70 [C-6]; 150.20 and 150.09 [C-4]; 146.4 [C-2]; 137.20-137.49 [m, C-1'']; 129.61-129.70 [m, C-2'']; 128.25-128.35 [m, C-3'']; 126.64-126.72 [m, C-4'']; 125.76 and 125.65 [C-8]; 124.45 and 124.43 [C-5]; 70.29-71.00 [m, C-3']; 67.16-68.66 [m, C-4', C-5']; 65.37 [C-6']; 60.49-60.73 [m, $CH_2CH_3$]; 53.72-54.40 [m, CH-NH]; 43.76 [C-1']; 39.7 [1''-$CH_2$]; 39.0 [C-2']; 29.7 [C-7']; 14.09-14.19 [m, $CH_3$]. HR-MS (ESI+) *m/z*: calcd for $C_{56}H_{71}BrN_8O_{13}P_2$ 1227.36914 $[M + Na]^+$, found 1227.36938 $[M + Na]^+$.

**Tetra-(L-phenylalanine ethylester) prodrug of {2-[3-(8-bromoguanin-9-yl)-2-(2-(bishydroxyphosphoryl)ethoxy)propoxy]ethyl}phosphonic acid (35)**

From compound **34** (171 mg, 0.15 mmol) according to **Method H**, afforded 24 mg (13%) of **35** as white lyophilisate.

$^1$H NMR (DMSO-$d_6$): 10.71 [bs, 1H, H-1]; 7.09-7.28 [m, 20H, H-2'', H-3'', H-4'']; 6.71 [bs, 2H, $NH_2$]; 4.42-4.57 [m, 2H, NH]; 4.06-4.18 [m, 2H, NH]; 3.78-4.04 [m, 14H, $CH_2CH_3$, H-1'; NH-CH]; 3.60 [m, 1H, H-2']; 3.18-3.42 [m, 6H, H-3', H-4', H-6']; 2.67-2.92 [m, 8H, 1''-$CH_2$]; 1.57-1.65 [m, 2H, H-5']; 1.43-1.51 [m, 2H, H-7']; 1.03-1.13 [m, 12H, $CH_3$]. $^{13}$C NMR (DMSO-$d_6$): 173.06-173.28 [m, COO]; 155.83 and 154.06 [C-2, C-6]; 152.87 [C-4]; 137.38-137.46 [m, C-1'']; 129.55-129.61 [m, C-2'']; 128.26-128.33 [m, C-3'']; 126.64-126.71 [m, C-4'']; 121.60 and 121.57 [C-8]; 116.85 and 116.82 [C-5]; 75.66 and 75.55 [C-2']; 69.64 and

69.43 [C-3']; 65.46 and 65.32 [C-4']; 64.48 and 64.42 [C-6']; 60.44-60.60 [m, $\underline{CH_2}CH_3$]; 53.89-54.46 [m, NH-$\underline{CH}$]; 44.82 and 44.76 [C-1']; 39.9 [1''-$CH_2$]; 29.63-30.77 [m, C-5', C-7']; 14.04-14.14 [m, $CH_3$]. HR-MS (ESI+) *m/z*: calcd for $C_{56}H_{72}BrN_9O_{13}P_2$ 1242.38004 $[M + Na]^+$, found 1242.38030 $[M + Na]^+$.

**Biological activity testing**

**Determination of $K_i$ values**. The $K_i$ values for the human and *Pf* enzymes were determined as previously described.[16,20] All assays were performed in 0.1 M Tris-HCl, 10 mM $MgCl_2$ at pH 7.4. Hanes' plots were determined at a fixed concentration of inhibitor and the non-variable substrate, guanine (49 μM). The concentration of *P*Rib-*PP* was varied between 20-1400 μM so that the maximum concentration of this substrate was at least four times that of $K_m$(app). The $K_i$ was calculated using the equation, $v_o = V_{max} .[S]_o/[S]_o + K_{m(app)}$ and $K_{m(app)} = K_m[1 + [I]/K_i]$. At [I]= 0 and the concentration of inhibitor used in the assay, $V_{max}$ was unchanged and the $K_m$ increased consistent with competitive inhibition. For inhibitors with low $K_i$ values (<2 μM), the $K_m$(app) was calculated at three different concentrations of inhibitor. These are single rates. The approximate $K_i$ values were calculated and were consistent with the final numbers. For these compounds, all of the plots are linear and parallel. The errors in $K_i$ value were calculated using GraphPad Prism. Standard deviations were derived by fitting all of the exeprimental data to $K_m(app) = K_m [1 + [I]/K_i]$.

**Crystallization and Structure Determination of Human HGPRT in complex with 20.** For crystallization experiments, human HGPRT was concentrated to 11.1 mg/mL (0.44 mM in terms of subunits). After concentration, the enzyme is stored at −70°C in 0.1 M Tris-HCl, 0.01 M $MgCl_2$, 1 mM DTT, and 300 μM PRib-PP, pH 7.4. Prior to crystallization, the enzyme was incubated with **20** for ~5 min to give a final concentration of the compound of 4.8 mM. For crystallization, the hanging drop method was used where 1 μL of reservoir

solution and 1 μL of human HGPRT in complex with the inhibitor were combined in the drops and incubated at 18°C. The reservoir solution for the complex was 20% PEG 3350, 0.2 M sodium bromide, 0.1 M Bis-tris propane, pH 7.5. Crystals were cryocooled in liquid nitrogen for shipment to the Australian Synchrotron where they were robotically placed in a cryostream (100 K) on beamline MX1. X-ray data were collected remotely using BLU-ICE.[28] All data sets were scaled and merged with XDS.[29] The structure was solved by molecular replacement using the program PHASER within PHENIX 1.8.[30] The protein coordinates of human HGPRT in complex with 9-[(N-phosphonoethyl-N-phosphonoethoxyethyl)-2-aminoethyl]-8-bromoguanine was the starting model (PDB code: 4RAB). Subsequent refinement and initial model building was with PHENIX 1.8 and COOT 0.8,[31] respectively.

***In vitro* antimalarial activity of ANbP prodrugs**. *P. falciparum* D6 (Sierra-Leone) laboratory line, sensitive to most antimalarial drugs and W2 (Indochina) line, resistant to chloroquine and pyrimethamine, were maintained as previously described[32] in RPMI-1640-LPLF complete medium, containing 10.4 g/l RPMI-1640-LPLF powder (Gibco BRL), 5.97 g/l HEPES buffer (MP Biomedicals, USA), 2.0 g/L D-glucose (BDH chemicals, Australia), 0.05 g/l hypoxanthine (Sigma, USA) and 40 mg/l gentamycin (Pfizer, Australia) with pH adjusted to 6.9. The sodium bicarbonate solution (0.21% final concentration) and human plasma (10% final) were added prior to use. Cultures were maintained at 4% hematocrit ($O(^{+})$ RBC) and 1% to 8% parasitemia at 37ºC in a special gas mixture (5% $O_2$, 5% $CO_2$ and 90% $N_2$). Cultures were routinely synchronized using D-sorbitol.[33] The antimalarial activity of the ANbPs was evaluated using the [$^3$H]-hypoxanthine growth inhibition assay.[34] For these assays, stock solutions of ANbPs were made to concentrations of 20-40 mM in DMSO or water and subsequently diluted in hypoxanthine-free complete media prior to assay. The assays (in 96-well plate format) were initiated when the majority of parasites (>90%) at early trophozoite (ring) stage. Parasite cultures (100 μl per well) at 0.5% initial parasitemia and 2%

hematocrit in hypoxanthine-free RPMI1640-LPLF medium were exposed to ten 2-fold serial dilutions of the ANbPs for 96 h, with [$^3$H]-hypoxanthine (0.2 μCi/well) added ~48 h after beginning of the experiment. The [$^3$H]-hypoxanthine incorporation data were analyzed and sigmoidal growth inhibition curves were produced by non-linear regression analysis of the [$^3$H]-hypoxanthine incorporation data versus log-transformed concentrations of the compounds using Graphpad Prism V5.0 software (GraphPad Software Inc. USA), from which the inhibitory concentration ($IC_{50}$) that cause 50% of parasite growth were determined. The $IC_{50}$ values were based on at least two independent experiments with mean (±SD) calculated.

**Cytotoxicity assays in human cell lines**. Human lung carcinoma A549 cells were seeded in 96-well plates at 7500 cells per well, and on the next day the compounds were added in serial dilutions. After four days incubation at 37°C, the cells were trypsinized, then counted with a Coulter Counter apparatus. The $CC_{50}$ or 50% cytostatic concentration, defined as the compound concentration producing 50% inhibition of cell proliferation as compared to the no compound control, was calculated by extrapolation assuming a semi-log dose-response effect.

## ASSOCIATED CONTENT

The atomic coordinates and structure factors of human HGPRT in complex with compound **20** have been deposited with the Protein Data Bank as entry 5W8V. Authors will release the atomic coordinates and experimental data upon article publication.

Supporting Information: SMILES strings of target ANbPs and their prodrugs

## CORRESPONDING AUTHOR INFORMATION

Dana Hockova: hockova@uochb.cas.cz

Luke W. Guddat.: luke.guddat@uq.edu.au

## ACKNOWLEDGEMENTS

Initial crystallographic conditions were determined using the University of Queensland Remote-Operation Crystallization and X-ray Diffraction facility (UQROCX). X-ray measurements were performed at the Australian Synchrotron. We thank Kerryn Rowcliffe for *in vitro* drug testing and the Australian Red Cross Blood Service for human blood. The views expressed here are those of the authors and not necessarily those of the Australian Synchrotron or the Australian Defence Organisation. This work was supported by NHMRC (Grant No. 1030353, to LWG, DH, and MDE), the Institute of Organic Chemistry and Biochemistry, RVO 61388963, the Czech Science Foundation (Grant No.16-06049S, to DH) and Gilead Sciences (Foster City, USA).

## ABBREVIATIONS

A549, human lung carcinoma cells; ACTs, artemisinin based combination therapies; ANbPs, acyclic nucleoside bisphosphonates; D6, *Plasmodium falciparum* strain sensitive to most drugs; DTT, dithiothreitol; HGPRT, hypoxanthine−guanine phosphoribosyltransferase; HGXPRT, hypoxanthine−guanine−xanthine phosphoribosyltransferase; HR, high resolution; IMP, inosine 5'-monophosphate; PDA, photodiode array; PEG, polyethylene glycol; *Pf*, *Plasmodium falciparum*; *Pv*, *Plasmodium vivax*; $PP_i$, pyrophosphate; RBC, red blood cell; RPMI1640-LPLF, Roswell Park Memorial Institute 1640 medium with low p-aminobenzoic acid and low folic acid; *P*Rib-*PP*, 5-phospho-*α*-D-ribosyl-1-pyrophosphate; TEAB, triethylammonium bicarbonate; Tris, 2-amino-2-(hydroxymethyl)propane-1,3-diol; UPLC, ultra performance liquid chromatography; W2, chloroquine- and pyrimethamine-resistant *Plasmodium falciparum* strain; XMP, xanthosine 5'-monophosphate.

## REFERENCES

(1) World Health Organization. *World Malaria Report 2016;* Geneva, Switzerland, 2016.

(2) Venkatesh, A.; Patel, S. K.; Ray, S.; Shastri, J.; Chatterjee, G.; Kochar, S. K.; Patankar, S.; Srivastava, S. Proteomics of *Plasmodium Vivax* Malaria: New Insights, Progress and Potential. *Expert Rev. Proteomics* **2016**, *13* (8), 771–782.

(3) Spring, M. D.; Lin, J. T.; Manning, J. E.; Vanachayangkul, P.; Somethy, S.; Bun, R.; Se, Y.; Chann, S.; Ittiverakul, M.; Sia-ngam, P.; Kuntawunginn, W.; Arsanok, M.; Buathong, N.; Chaorattanakawee, S.; Gosi, P.; Ta-aksorn, W.; Chanarat, N.; Sundrakes, S.; Kong, N.; Heng, T. K.; Nou, S.; Teja-isavadharm, P.; Pichyangkul, S.; Phann, S. T.; Balasubramanian, S.; Juliano, J. J.; Meshnick, S. R.; Chour, C. M.; Prom, S.; Lanteri, C. A.; Lon, C.; Saunders, D. L. Dihydroartemisinin-piperaquine Failure Associated with a Triple Mutant Including *Kelch13 C580Y* in Cambodia: An Observational Cohort Study. *Lancet Infect. Dis.* **2015**, *15*, 621-623.

(4) Thanh, N. V.; Thuy-Nhien, N.; Tuyen, N. T. K.; Tong, N. T.; Nha-Ca, N. T.; Dong, L. T.; Quang, H. H.; Farrar, J.; Thwaites, G.; White, N. J.; Wolbers, M.; Hien, T. T. Rapid Decline in the Susceptibility of *Plasmodium falciparum* to Dihydroartemisinin-piperaquine in the South of Vietnam. *Malaria J.* **2017**, *16*, 27.

(5) Cassera, M. B.; Zhang, Y.; Hazleton, K. Z.; Schramm, V. L. Purine and Pyrimidine Pathways as Targets in Plasmodium falciparum. *Curr. Top. Med. Chem.* **2011**, *11* (16), 2103-2115.

(6) Berman, P. A.; Human, L. Hypoxanthine Depletion Induced by Xanthine Oxidase Inhibits Malaria Parasite Growth *in vitro*. *Purine and Pyrimidine Metabolism in Man VII: Part A: Chemotherapy, ATP Depletion, and Gout*; Harkness, R. A., Elion, G. B., Zöllner, N., Eds.; Plenum Press: New York and London, **1991**; pp 165–168.

(7) Keough, D. T.; Hocková, D.; Holý, A.; Naesens, L. M. J.; Skinner-Adams, T. S.; De

Jersey, J.; Guddat, L. W. Inhibition of Hypoxanthine-Guanine Phosphoribosyltransferase by Acyclic Nucleoside Phosphonates: A New Class of Antimalarial Therapeutics. *J. Med. Chem.* **2009**, *52* (14), 4391–4399.

(8) Li, C. M.; Tyler, P. C.; Furneaux, R. H.; Kicska, G.; Xu, Y.; Grubmeyer, C.; Girvin, M. E.; Schramm, V. L. Transition-State Analogs as Inhibitors of Human and Malarial Hypoxanthine-Guanine Phosphoribosyltransferases. *Nat. Struct. Mol. Biol.* **1999**, *6*, 582–587.

(9) Ducati, R. G.; Namanja-Magliano, H. A.; Schramm, V. L. Transition-State Inhibitors of Purine Salvage and Other Prospective Enzyme Targets in Malaria. *Future Med. Chem.* **2013**, *5* (11), 1341–1360.

(10) Clinch, K.; Crump, D. R.; Evans, G. B.; Hazleton, K. Z.; Mason, J. M.; Schramm, V. L.; Tyler, P. C. Acyclic Phosph(on)ate Inhibitors of *Plasmodium Falciparum* Hypoxanthine-Guanine-Xanthine Phosphoribosyltransferase. *Bioorganic Med. Chem.* **2013**, *21* (17), 5629–5646.

(11) Terán, D.; Hocková, D.; Česnek, M.; Zíková, A.; Naesens, L.; Keough, D. T.; Guddat, L. W. Crystal Structures and Inhibition of *Trypanosoma Brucei* Hypoxanthine–guanine Phosphoribosyltransferase. *Sci. Rep.* **2016**, *6*, 35894.

(12) Eng, W. S.; Hocková, D.; Špaček, P.; Janeba, Z.; West, N. P.; Woods, K.; Naesens, L. M. J.; Keough, D. T.; Guddat, L. W. First Crystal Structures of *Mycobacterium Tuberculosis* 6-Oxopurine Phosphoribosyltransferase: Complexes with GMP and Pyrophosphate and with Acyclic Nucleoside Phosphonates Whose Prodrugs Have Antituberculosis Activity. *J. Med. Chem.* **2015**, *58* (11), 4822–4838.

(13) Keough, D. T.; Hocková, D.; Krečmerová, M.; Česnek, M.; Holý, A.; Naesens, L.; Brereton, I. M.; Winzor, D. J.; de Jersey, J.; Guddat, L. W. *Plasmodium Vivax* Hypoxanthine-Guanine Phosphoribosyltransferase: A Target for Anti-Malarial

Chemotherapy. *Mol. Biochem. Parasitol.* **2010**, *173* (2), 165–169.

(14) Keough, D. T.; Hocková, D.; Janeba, Z.; Wang, T. H.; Naesens, L.; Edstein, M. D.; Chavchich, M.; Guddat, L. W. Aza-Acyclic Nucleoside Phosphonates Containing a Second Phosphonate Group as Inhibitors of the Human, *Plasmodium Falciparum* and *Vivax* 6-Oxopurine Phosphoribosyltransferases and Their Prodrugs as Antimalarial Agents. *J. Med. Chem.* **2015**, *58* (2), 827–846.

(15) Keough, D. T.; Hocková, D.; Rejman, D.; Špaček, P.; Vrbková, S.; Krečmerová, M.; Eng, W. S.; Jans, H.; West, N. P.; Naesens, L. M. J.; De Jersey, J.; Guddat, L. W. Inhibition of the *Escherichia Coli* 6-Oxopurine Phosphoribosyltransferases by Nucleoside Phosphonates: Potential for New Antibacterial Agents. *J. Med. Chem.* **2013**, *56* (17), 6967–6984.

(16) Keough, D. T.; Špaček, P.; Hocková, D.; Tichý, T.; Vrbková, S.; Slavětínská, L.; Janeba, Z.; Naesens, L.; Edstein, M. D.; Chavchich, M.; Wang, T. H.; De Jersey, J.; Guddat, L. W. Acyclic Nucleoside Phosphonates Containing a Second Phosphonate Group Are Potent Inhibitors of 6-Oxopurine Phosphoribosyltransferases and Have Antimalarial Activity. *J. Med. Chem.* **2013**, *56* (6), 2513–2526.

(17) Česnek, M.; Hocková, D.; Holý, A.; Dračínský, M.; Baszczyňski, O.; Jersey, J. De; Keough, D. T.; Guddat, L. W. Synthesis of 9-Phosphonoalkyl and 9-Phosphonoalkoxyalkyl Purines: Evaluation of Their Ability to Act as Inhibitors of *Plasmodium Falciparum, Plasmodium Vivax* and Human Hypoxanthine-Guanine-(Xanthine) Phosphoribosyltransferases. *Bioorg. Med. Chem.* **2012**, *20* (2), 1076–1089.

(18) Thornton, P. J.; Kadri, H.; Miccoli, A.; Mehellou, Y. Nucleoside Phosphate and Phosphonate Prodrug Clinical Candidates. *J. Med. Chem.* **2016**, *59* (23), 10400–10410.

(19) Hocková, D.; Janeba, Z.; Naesens, L.; Edstein, M. D.; Chavchich, M.; Keough, D. T.; Guddat, L. W. Antimalarial Activity of Prodrugs of N-Branched Acyclic Nucleoside

Phosphonate Inhibitors of 6-Oxopurine Phosphoribosyltransferases. *Bioorg. Med. Chem.* **2015**, *23* (17), 5502–5510.

(20) Špaček, P.; Keough, D. T.; Chavchich, M.; Dračínský, M.; Janeba, Z.; Naesens, L.; Edstein, M. D.; Guddat, L. W.; Hocková, D. Synthesis and Evaluation of Symmetric Acyclic Nucleoside Bisphosphonates as Inhibitors of the *Plasmodium Falciparum, Plasmodium Vivax* and Human 6-Oxopurine Phosphoribosyltransferases and the Antimalarial Activity of Their Prodrugs. *Bioorg. Med. Chem.* **2017**, *25*, 4008-4030.

(21) Baszczyňski, O.; Jansa, P.; Dračínský, M.; Kaiser, M. M.; Špaček, P.; Janeba, Z. An Efficient Oxa-Michael Addition to Diethyl Vinylphosphonate under Mild Reaction Conditions. *RSC Adv.* **2012**, *2* (4), 1282–1284.

(22) Thompson, D. H.; Boomer, J. A.; Haynes, R. Vinyl Ether Lipids with Cleavable Hydrophlic Headgroups. U.S. Patent 6,979,460 B1, Dec 27, 2005.

(23) Linn, J. A.; McLean, E. W.; Kelley, J. L. 1,4-Diazabicyclo[2.2.2]octane (Dabco)-Catalysed Hydrolysis and Alcoholysis Reactions of 2-Amino-9-Benzyl-6-Chloro-9H-Purine. *J. Chem. Soc. Commun.* **1994**, *8* (8), 913–914.

(24) de Jersey, J.; Holý, A.; Hocková, D.; Naesens, L.; Keough, D. T.; Guddat, L. W. 6-Oxopurine Phosphoribosyltransferase: A Target for the Development of Antimalarial Drugs. *Curr. Top. Med. Chem.* **2011**, *11* (16), 2085–2102.

(25) Kaiser, M. M.; Hocková, D.; Wang, T.-H.; Dračínský, M.; Poštová-Slavětínská, L.; Procházková, E.; Edstein, M. D.; Chavchich, M.; Keough, D. T.; Guddat, L. W.; Janeba, Z. Synthesis and Evaluation of Novel Acyclic Nucleoside Phosphonates as Inhibitors of *Plasmodium Falciparum* and Human 6-Oxopurine Phosphoribosyltransferases. *ChemMedChem* **2015**, *10* (10), 1707–1723.

(26) Jansa, P.; Baszczyňski, O.; Dračínský, M.; Votruba, I.; Zídek, Z.; Bahador, G.; Stepan, G.; Cihlar, T.; MacKman, R.; Holý, A.; Janeba, Z. A Novel and Efficient One-Pot

Synthesis of Symmetrical Diamide (Bis-Amidate) Prodrugs of Acyclic Nucleoside Phosphonates and Evaluation of Their Biological Activities. *Eur. J. Med. Chem.* **2011**, *46* (9), 3748–3754.

(27) Shi, W.; Li, C. M.; Tyler, P. C.; Furneaux, R. H.; Cahill, S. M.; Girvin, M. E.; Grubmeyer, C.; Schramm, V. L.; Almo, S. C. The 2.0 Å Structure of Human Hypoxanthine-Guanine Phosphoribosyltransferase in Complex with a Transition-State Analog Inhibitor. *Nat. Struct. Biol.* **1999**, *6* (6), 588–593.

(28) McPhillips, T. M.; McPhillips, S. E.; Chiu, H.-J.; Cohen, A. E.; Deacon, A. M.; Ellis, P. J.; Garman, E.; Gonzalez, A.; Sauter, N. K.; Phizackerley, R. P.; Soltis, S. M.; Kuhn, P. *Blu-Ice* and the *Distributed Control System*: Software for Data Acquisition and Instrument Control at Macromolecular Crystallography BeamLines. *J. Synchrotron Radiat.* **2002**, *9* (6), 401–406.

(29) Kabsch, W. XDS. *Acta Crystallogr. Sect. D* **2010**, *66* (2), 125–132.

(30) Adams, P. D.; Afonine, P. V; Bunkóczi, G.; Chen, V. B.; Davis, I. W.; Echols, N.; Headd, J. J.; Hung, L.-W.; Kapral, G. J.; Grosse-Kunstleve, R. W.; McCoy, A. J.; Moriarty, N. W.; Oeffner, R.; Read, R. J.; Richardson, D. C.; Richardson, J. S.; Terwilliger, T. C.; Zwart, P. H. *PHENIX*: A Comprehensive Python-Based System for Macromolecular Structure Solution. *Acta Crystallogr. Sect. D* **2010**, *66* (2), 213–221.

(31) Emsley, P.; Lohkamp, B.; Scott, W. G.; Cowtan, K. Features and Development of Coot. *Acta Crystallogr. Sect. D* **2010**, *66* (4), 486–501.

(32) Trager, W.; Jensen, J. B. Human Malaria Parasites in Continuous Culture. *Science* **1976**, *193* (4254), 673–675.

(33) Lambros, C.; Vanderberg, J. P. Synchronization of *Plasmodium falciparum* Erythrocytic Stages in Culture. *J. Parasitol.* **1979**, *65* (3), 418–420.

(34) Desjardins, R. E.; Canfield, C. J.; Haynes, J. D.; Chulay, J. D. Quantitative Assessment

of Antimalarial Activity *in vitro* by a Semiautomated Microdilution Technique. *Antimicrob. Agents Chemother.* **1979**, *16* (6), 710–718.

**For Table of Contents Only**

**TOC Graphic:**